

Rainfall and erosivity in the municipality of Rio de Janeiro - Brazil

Paulo Miguel de Bodas Terassi^{a,*}, José Francisco de Oliveira-Júnior^{b,f}, Givanildo de Gois^c, Antonio Carlos Oscar Júnior^d, Bruno Serafini Sobral^{e,f}, Vitor Hugo Rosa Biffi^g, Claudio José Cavalcante Blanco^h, Washington Luiz Félix Correia Filho^b, Hamza Vijithⁱ



^a Postgraduate Program in Physical Geography, University of São Paulo, Professor Lineu Prestes avenue, 338, CEP: 05508-000, Cidade Universitária, São Paulo, Brazil

^b Institute of Atmospheric Sciences, Federal University of Alagoas, Lourival Melo Mota avenue, S/N, CEP: 57072-970, Tabuleiro dos Martins, Maceió, Alagoas, Brazil

^c School of Industrial Metallurgical Engineering of Volta Redonda, Technological Center, Federal Fluminense University, Trabalhadores avenue, 420, CEP:27255-250, Vila Santa Cecília, Cidade Universitária, Volta Redonda, Rio de Janeiro, Brazil

^d Department of Physical Geography, Rio de Janeiro State University, São Francisco Street, 524, CEP:20550-900, Maracanã, Rio de Janeiro, Brazil

^e Land and Cartography Institute of Rio de Janeiro (ITERJ), State Secretary for the Environment and Sustainability (SEA-RJ), Rua Regente Feijó, 7, Centro, Rio de Janeiro 20060-060, Brazil

^f Postgraduate Program in Biosystems Engineering (PGEB), Federal Fluminense University (UFF), Passo da Pátria street, 156, CEP: 24210-240, São Domingos, Niterói, Rio de Janeiro, Brazil

^g Postgraduate Program in Geography, State University of Western Paraná, Maringá street, 1200, CEP: 85605-010, Vila Nova, Francisco Beltrão, Paraná, Brazil

^h Postgraduate Program in Civil Engineering, Federal University of Pará, Rua Augusto Corrêa, 1, CEP:66075-110, Guatá, Belém, Brazil

ⁱ Department of Applied Geology, Faculty of Engineering and Science, Curtin University, Miri, Malaysia

ARTICLE INFO

Keywords:

Rainfall erosivity

Urban areas

Rio de Janeiro

Statistical analyses

Isohyetal

ABSTRACT

This study analyzes spatio-temporal variability and erosion potential related to rainfall in the municipality of Rio de Janeiro (MRJ), considering the period of 1997 to 2016. The rainfall series of *Alerta Rio* system were used, which is composed of 33 rainfall stations. To establish the values of the erosivity index, a linear eq. ($Y = a + bx$) was used. Ordinary kriging and clustering techniques were used for the spatial analysis of rainfall and erosivity, and the time series were evaluated using parametric tests (Bartlett and Shapiro-Wilk) and descriptive statistics (mean, median, variance, asymmetry, kurtosis and quartiles). It was observed that about 85% of the annual average erosivity is concentrated between the period of September and April, corresponding to the period of greatest probability for erosion impacts occurrence. Results revealed a spatial structure in rainfall, which is directly associated with physiographic aspects of the MRJ and the impacts resulting from urbanization. The Shapiro-Wilk test indicated the predominance of non-significant results for the months of February and November, which is associated to the frequent occurrence of dry spells, atmosphere blockages (February) and transition between the dry and rainy seasons (November).

* Corresponding author.

E-mail addresses: pmbterassi@usp.br (P.M.d.B. Terassi), antonio.junior@uerj.br (A.C. Oscar Júnior).

1. Introduction

Knowledge of the rainfall spatio-temporal distribution is essential for the planning of numerous public activities and influences in areas such as forestry, agriculture, water resources, energy generation, trade, tourism, air quality, urban drainage and development (Dereczynski et al., 2009; Amorim and Monteiro, 2010; Zeri et al., 2011; Brito et al., 2016).

Shastri et al. (2015) point out that studies addressing the spatial and temporal characteristics of rainfall allow us to subsidize key sectors to minimize rainfall impacts in urban areas, especially in large metropolises. These cities are greatly impacted by events of floods, mass movements, food and water shortages, dislodgments and, even, fatalities. According to Armond and Sant'anna Neto (2017), extreme rainfall events cause disruptive situations and disturb the environment of metropolises, while also emphasizing that urban disorder originated from the influence of rainfall does not necessarily occur by great events of rainfall, but also by physical factors and socioeconomic conditions, sometimes combined.

Water erosion caused by rainfall is considered a major environmental problem, which can lead to mass movements derived from excessive rainfall. The rainfall potential to cause soil erosion is termed erosivity (Shamshad et al., 2008; Mello et al., 2013; Oliveira et al., 2013). Knowledge of rainfall erosivity is essential for the prediction of soil losses by water erosion (Silva et al., 2011; Almeida et al., 2012) and is therefore essential to evaluate the environmental impacts of agricultural practices and the control of erosion, while also subsidizing civil engineering works, such as bridges and dams (Bazzano et al., 2007). Specifically, the municipality of Rio de Janeiro (MRJ) registers almost every year many problems caused by extreme and concentrated rains, which cause accelerated erosion and landslides.

Spatial analysis allows the identification of sectors that are most vulnerable to the erosive potential of rainfall and, consequently, greater attention to the originated impacts, such as loss of soil fertility, river silting and mass movements (Hoyos et al., 2005), and in the literature (Shastri et al., 2015). Therefore, the temporal identification of erosivity establishes the periods of greater susceptibility to the previously mentioned environmental impacts and, whithat, subsidizes the agricultural, environmental and territorial planning (Ma et al., 2012; Back et al., 2018).

Studies on rainfall erosivity in the Brazilian territory are not uncommon due to the economic importance of agribusiness and the predominant characteristics of rainfall. These are proper to the humid and subhumid tropical climate that covers most of the country (76%), as well as the subtropical climate (14%), according to the classification of Álvares et al. (2013), which present annual rainfall above 1000 mm and, according to Panagos et al. (2017), correspond to the climatic types in which the highest Earth Globe erosivity rates occur. Silva (2004) verified that 69% of Brazil has high or very high erosivity ($> 7357 \text{ MJ.mm.h}^{-1}.\text{year}^{-1}$), concentrated mainly in the months of December and January and less intense between June and September. Trindade et al. (2016) observed that 56% of Brazil presents high or very high erosivity and that between November and March the highest rates of erosivity occur in almost all Brazilian territory. In Rio de Janeiro state, where MRJ is located, works of Brito et al. (2016) and Sobral et al. (2018) confere to these periods the greatest incidence of rainfall.

Montebeller et al. (2007) performed the spatial analysis of erosivity for the State of Rio de Janeiro (SRJ) and identified that the highest annual values were identified for the Mountainous region and the bay of Ilha Grande, with a predominance of values higher than $8000 \text{ MJ.mm.h}^{-1}.\text{year}^{-1}$, classifying these regions as the most susceptible to erosive potential. Opposingly, the northeast of the state presents erosivity below $4000 \text{ MJ.mm.h}^{-1}.\text{year}^{-1}$. Using artificial neural networks, the mapping of Carvalho et al. (2012) showed the validity of the results obtained previously by the previous cited authors, highlighting the role of geographic characteristics such as altitude, latitude and longitude for the spatial distribution of isohyets in the SRJ.

Previous studies have emphasized the relevance of the investigation of the pluviometric characteristics of Brazilian cities and their associations with urban space disorder, such as Zanella (2006) for Curitiba (PR), Zanella and Salles (2016) for Fortaleza, Souza et al. (2012) for Recife, Costa and Blanco (2018) for Belém and Fialho and Brandão (2000) and Armond and Sant'anna Neto (2017) for Rio de Janeiro. However, no other estimates were made for rainfall erosion potential and its spatialisation in a Brazilian metropolis, especially Rio de Janeiro, with great population density (Moraes et al., 2005; Zeri et al., 2011) that often suffer negative impacts derived from rainfall. Therefore, this study analyzes rainfall spatio-temporal variability and the erosive potential of rainfall in the MRJ using data from the period of 1997 to 2016.

2. Material and methods

2.1. Study area

The MRJ is located between parallels $22^{\circ} 45' 05'' \text{S}$ and $23^{\circ} 04' 10'' \text{S}$ and the meridians $43^{\circ} 06' 30'' \text{W}$ and $43^{\circ} 47' 40'' \text{W}$. It is delimited to the north (N) by the municipalities of Itaguaí, Seropédica, Nova Iguaçu, Nilópolis, Mesquita, São João de Meriti and Duque de Caxias; to the east (E) by the Guanabara's Bay and to the south by the Atlantic Ocean (Fig. 1).

The MRJ area is home to approximately 6320,446 inhabitants and covers an area of $1,200,179 \text{ km}^2$ (Ibge (Instituto Brasileiro de Geografia e Estatística), 2018). Among its physical characteristics, the hilly topography is extremely diverse, marked by the formation of massifs, whose steep slopes were originally covered by the Atlantic Forest. The main massifs within the MRJ are Gericinó - Mendenha, to the north, where are located the sierras of the same name with altitudes of 887 m and 974 m, respectively; Pico do Guandu located at 964 m of altitude; Tijuca, to the east, with up to 1022 m altitude; and the Pedra Branca massif to the west, where the highest point of the MRJ is located, the Pedra Branca Peak at 1025 m (Dereczynski et al., 2009).

According to official data acquired from the Inmet (Instituto Nacional de Meteorologia) (2018) historic series for the MRJ from 1961 to 1990, annual rainfall in the city registers an average of 1069.2 mm/year. The average annual temperature is 23.8°C (Inmet

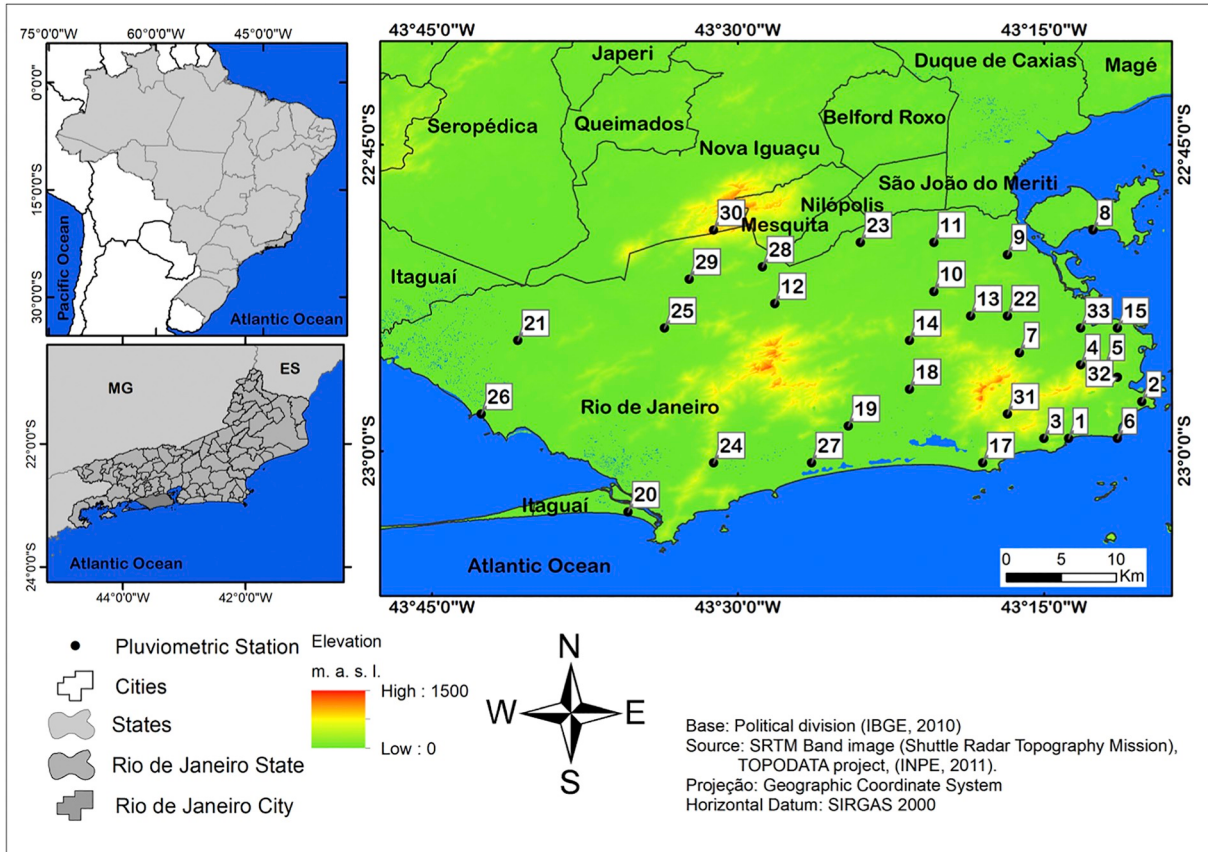


Fig. 1. Geographic location of rainfall stations in the municipality of Rio de Janeiro, Brazil.

(Instituto Nacional de Meteorologia), 2018). The warmest period occurs between January and March, with an average temperature above 26 °C. The lowest temperatures are recorded between May and July, and are frequently around 22 °C. The rainy season occurs between December and March, with monthly averages of rainfall totals above 100 mm. The driest months in the MRJ (< 50 mm) usually occur along with the winter season, being June and August the months of the year with greatest frequency of drought occurrence. These characteristics confer to the MRJ the climatic type “Aw” - hot tropical with dry winters - agreeing to the conclusions verified by Alvares et al. (2013) and Dubreuil et al. (2017) for this sector of the State of Rio de Janeiro (SRJ).

2.2. Rainfall historical series

Rainfall series considering the period from 1997 to 2016 were acquired from the “Sistema Alerta Rio” database - Alerta Rio (<http://alertario.rio.rj.gov.br/>) - considering 33 rainfall stations (Table 1). These database was used to evaluate the spatio-temporal characteristics of rainfall and to perform the erosivity estimates for the MRJ.

Monthly series were then analyzed for data quality control (percentage of failures) and the completion of data faults, for which the regional weighting method was applied, as presented by Villela and Mattos (1975). This method is based on rainfall records of three stations located as close as possible to the station where the lack of data is to be filled, selecting rainfall stations with similar temporal characteristics (monthly and annual distribution) and altitudes (Oliveira et al., 2010).

2.3. Calculation of erosivity estimates

The erosivity index was calculated based on the monthly and annual average data of the 33 pluviometric stations. In order to establish the values of the monthly erosivity index (EI_m), the equation of type $Y = a + bx$ was used, where: Y = erosion index ($MJ \cdot mm \cdot ha^{-1} \cdot h^{-1} \cdot year^{-1}$); a and b = linear and angular coefficients; and $x = p^2 / P$ (p - monthly squared rainfall divided by the annual rainfall - P). Equation (Eq. 1) defined by Gonçalves et al. (2006) was used, since it has been defined by these authors as the better linear correlation between rainfall and erosivity for the MRJ.

$$EI_m = 3.89 + 37.76 \left(\frac{p^2}{P} \right)^{0.80665} \quad (1)$$

Table 1
Location, altitude and data faults of the pluviometric stations.

ID	Pluviometric station	Latitude (°)	Longitude (°)	Altitude (m)	Data faults (%)
1	Vidigal	-22.99	-43.23	85	0.0
2	Urca	-22.96	-43.17	90	0.0
3	Rocinha	-22.99	-43.25	160	0.0
4	Tijuca	-22.93	-43.22	340	0.0
5	Santa Teresa	-22.93	-43.20	170	0.0
6	Copacabana	-22.99	-43.19	90	0.0
7	Grajaú	-22.92	-43.27	80	0.0
8	Ilha do Governador	-22.82	-43.21	0	0.0
9	Penha	-22.84	-43.28	111	0.0
10	Madureira	-22.87	-43.34	45	0.0
11	Irajá	-22.83	-43.34	20	0.0
12	Bangu	-22.88	-43.47	15	0.0
13	Piedade	-22.89	-43.31	50	0.0
14	Jacarepaguá/Tanque	-22.91	-43.36	73	0.0
15	Saúde	-22.90	-43.19	15	0.0
16	Jardim Botânico	-22.97	-43.22	0	0.0
17	Barra/Barrinha	-23.01	-43.30	7	0.0
18	Jacarepaguá/Cidade de Deus	-22.95	-43.36	15	0.0
19	Barra/Riocentro	-22.98	-43.41	0	0.0
20	Guaratiba	-23.05	-43.59	0	0.0
21	Santa Cruz	-22.91	-43.68	15	0.0
22	Grande Méier	-22.89	-43.28	25	0.0
23	Anchieta	-22.83	-43.40	50	0.0
24	Grota Funda	-23.01	-43.52	11	0.0
25	Campo Grande	-22.90	-43.56	30	0.0
26	Sepetiba	-22.97	-43.71	62	0.0
27	Recreio dos Bandeirantes	-23.01	-43.44	10	0.0
28	Gericinó	-22.52	-43.35	30	33.33
29	Av. Brasil/Mendanha	-22.86	-43.54	30	20.00
30	Mendanha	22.82	43.52	736	34.17
31	Alto da Boa Vista	-22.97	-43.28	355	20.00
32	Laranjeiras	-22.94	-43.19	60	20.00
33	São Cristóvão	-22.90	-43.22	25	20.00

where: EI_m – Monthly erosion index in MJ (MJ.mm.ha $^{-1}$.h $^{-1}$.year $^{-1}$); a – linear coefficient; b – angular coefficient; p – Monthly average rainfall (mm); P – Annual average rainfall (mm); 980,665 – Conversion of kgf (kilogram force) to MJ (Megajoule).

2.4. Parametric tests of Shapiro-Wilk (SW) and Bartlett (B)

The SW test was applied to the time series according to a normal probability distribution. It consists of the ratio of two distinct estimators of variance. The numerator estimator is based on a linear combination of quantities, and related to the normal distribution, and the denominator estimator was obtained by the conventional way.

The test statistic of SW (W) is defined by Eq. 2 given by:

$$W = \frac{\left[\sum_{i=1}^k a_{n-i+1} (y_{n-i+1} - \bar{y}_i) \right]^2}{\sum_{i=1}^n (y_i - \bar{y})^2} = \frac{\left[\sum_{i=1}^k a_i y_{(i)} \right]^2}{\sum_{i=1}^n (y_i - \bar{y})^2} \quad (2)$$

where, $i = 1, 2, n$, is the sample size; y_i = measurement value of the sample under analysis, ordered from lowest to highest; \bar{y} = the average value of the measurement; a_i = coefficient generated from variances and covariates of the statistical order of a sample of size n and a normal distribution.

Where X is the analyzed variable, we formulate the hypotheses:

H_0 : The rainfall data of the stations present residues with normal distribution (Gaussian);

H_1 : The rainfall data of the stations do not present residues with normal distribution (Gaussian).

The conditions for the data to be distributed according to a normal distribution at probability level α (5%) are:

For $W_{cal} \leq W_{tab}$ reject H_0 to P.value $\alpha < 0,05$ (Significant - S);

For $W_{cal} \geq W_{tab}$ accept H_0 to P.value $\alpha > 0,05$ (Non-significant - NS).

The Bartlett test (1937) was used to verify the assumption that K samples from a population have equal variances (homogeneity of variances). The Bartlett test statistic is defined by B_0 using the following equations:

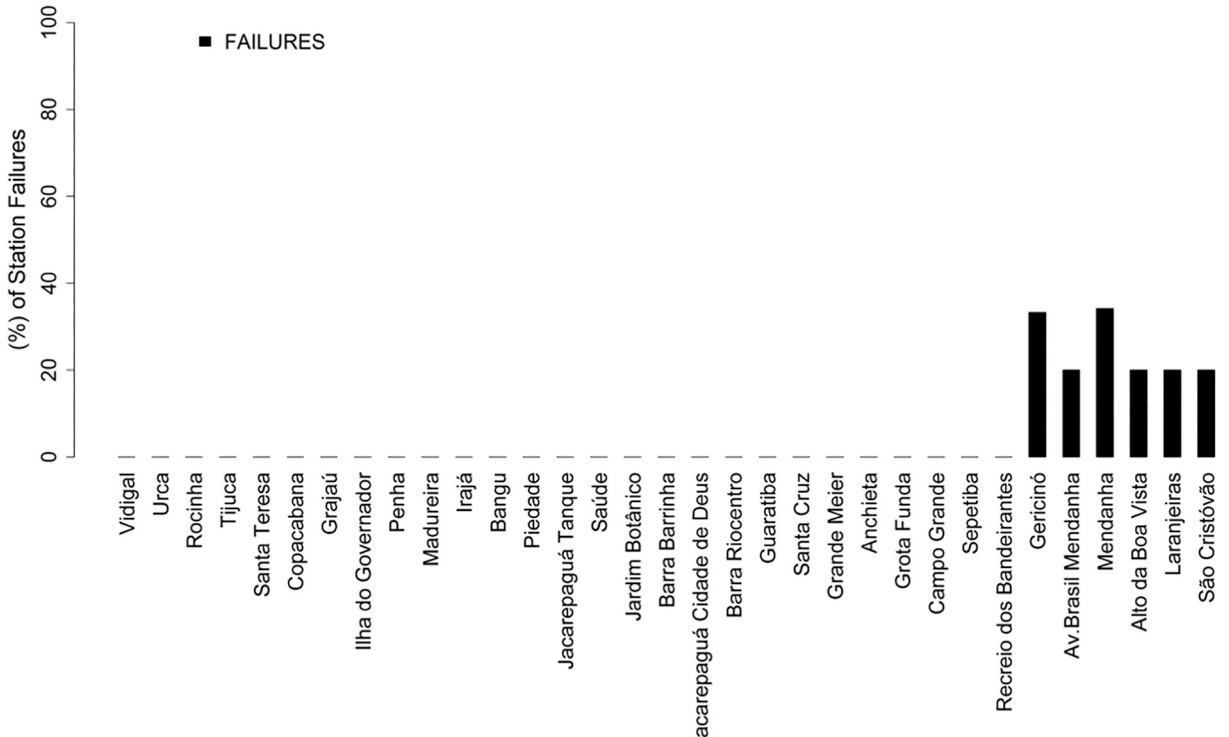


Fig. 2. Spatial distribution of rainfall (a) in the annual scale for the municipality of Rio de Janeiro, Brazil.

$$N = \sum_{j=1}^n n_j \quad (3)$$

$$S_i^2 = \sum_{j=1}^{n_i} \frac{(y_{ij} - \bar{y}_i)^2}{n_i - 1} \quad (4)$$

$$S_p^2 = \frac{1}{N - k} \sum_{i=1}^k (n_i - 1) S_i^2 \quad (5)$$

$$q = (N - k) \ln S_p^2 - \sum_{i=1}^k [(n_i - 1) \ln S_i^2] \quad (6)$$

$$c = 1 + \frac{1}{3(k-1)} \left(\sum_{i=1}^n \frac{1}{n_i - 1} - \frac{1}{N - k} \right) \quad (7)$$

where B_0 is defined as:

$$B_0 = \frac{q}{c} \quad (8)$$

B_0 over the hypothesis $H_0 \approx \chi_{k-1}^2$.

Where, N = number of observations, n_i e k = number of observations within groups, S_i^2 = sample variance, S_p^2 = population variance, q = numerator coefficient, c = denominator coefficient, χ_{k-1}^2 = chi-square distribution, a significance level and B_0 = Bartlett's test statistics.

Being X the most analyzed variable, the following hypothesis were formulated:

H_0 : Rainfall data presents homogeneous variances;

H_1 : Rainfall data do not present homogeneous variances.

The conditions for the data to show homogeneity or heterogeneity of variances at the probability level α are:

For $B_0 \geq \chi_{(1-\alpha, k-1)}^2$ reject H_0 to P-value $\alpha < 0,05$ (Significant - S);

For $B_0 \leq \chi_{(1-\alpha, k-1)}^2$ accept H_0 to P-value $\alpha > 0,05$ (Non-significant - NS).

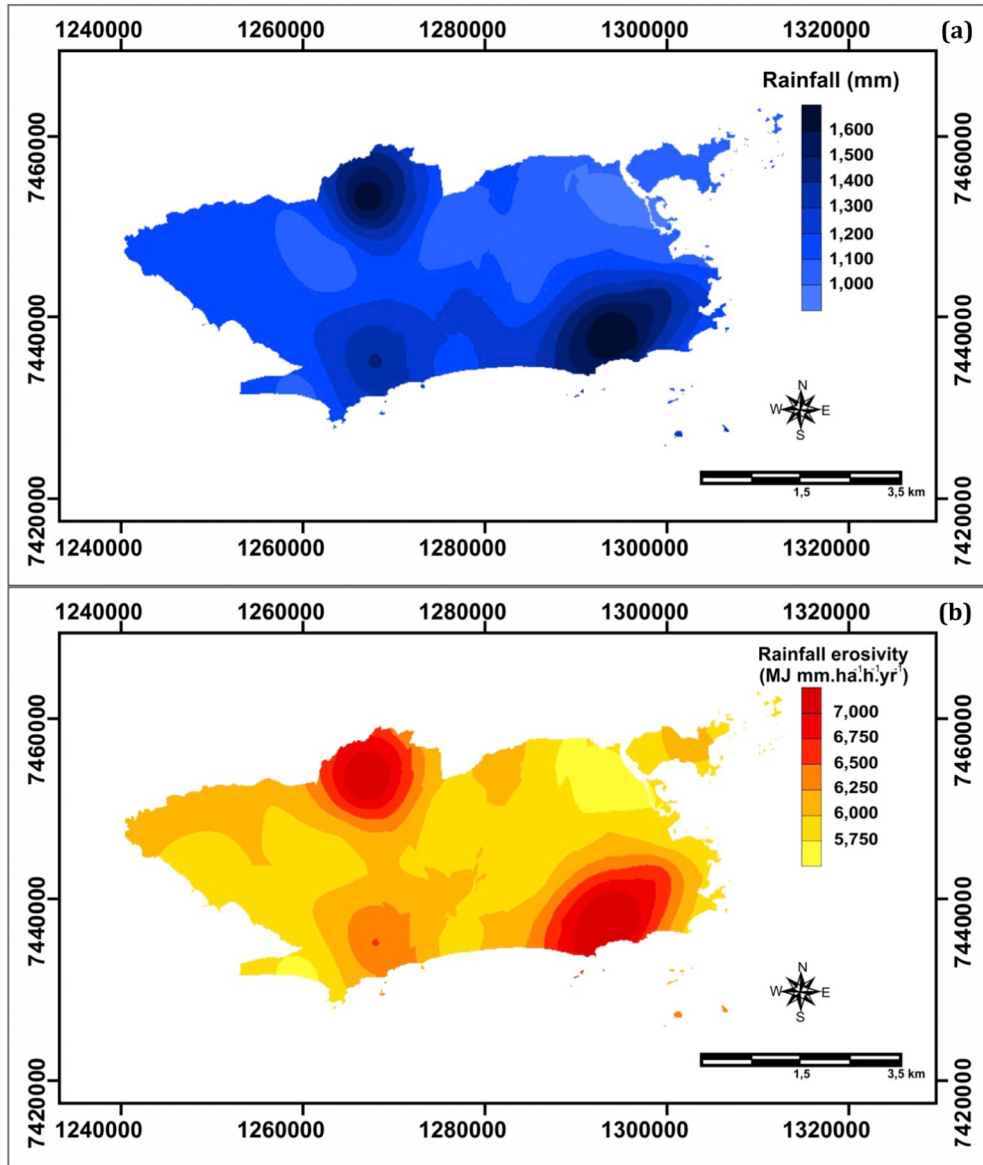


Fig. 3. Spatial distribution of rainfall in the months of January (a), February (b), March (c), April (d), May (e), June (f), July (g), August (h), September (i), October (j), November (k) and December (l) in the municipality of Rio de Janeiro, Brazil.

2.5. Spatial analysis (Kriging and clustering)

For the elaboration of rainfall charts ArcGIS software version 10.3 was used. Combining the shapefile of the study area with rainfall values registered by the stations within the MRJ, annual and monthly rainfall and erosivity maps were created. The interpolation of the data was completed using the Ordinary Kriging method, which allows more adequate representation rainfall, as pointed out by [Carvalho and Assad \(2005\)](#), [Gois et al. \(2015\)](#) and [Mello and Oliveira \(2016\)](#).

As the present research showed a significant number of pluviometric stations, was performed an experimental semivariogram test to verify the association of the Nugget Effect variograph model with the Exponential and or Spherical model was the most appropriate for the selected kriging options. These associations demonstrated the lowest number of isohyets and isoerodents and the intervals generated for these isolates were the closest to the real values of the maximum and minimum intervals for rain and erosivity. Statistically, it was observed that kriging interpolation obtained a spatial correlation predominantly greater than 0.8.

Cluster analysis (CA) was applied to the time series of rainfall data. Thus, the respective numbers of groups and the dendrogram were determined. The number of groups adopted and the stratification of the stations was based on Ward's agglomerative hierarchical method (1963), considering as a measure of dissimilarity the Euclidian distance ([Everitt and Dunn, 1991](#)).

The Euclidian distance is given by:

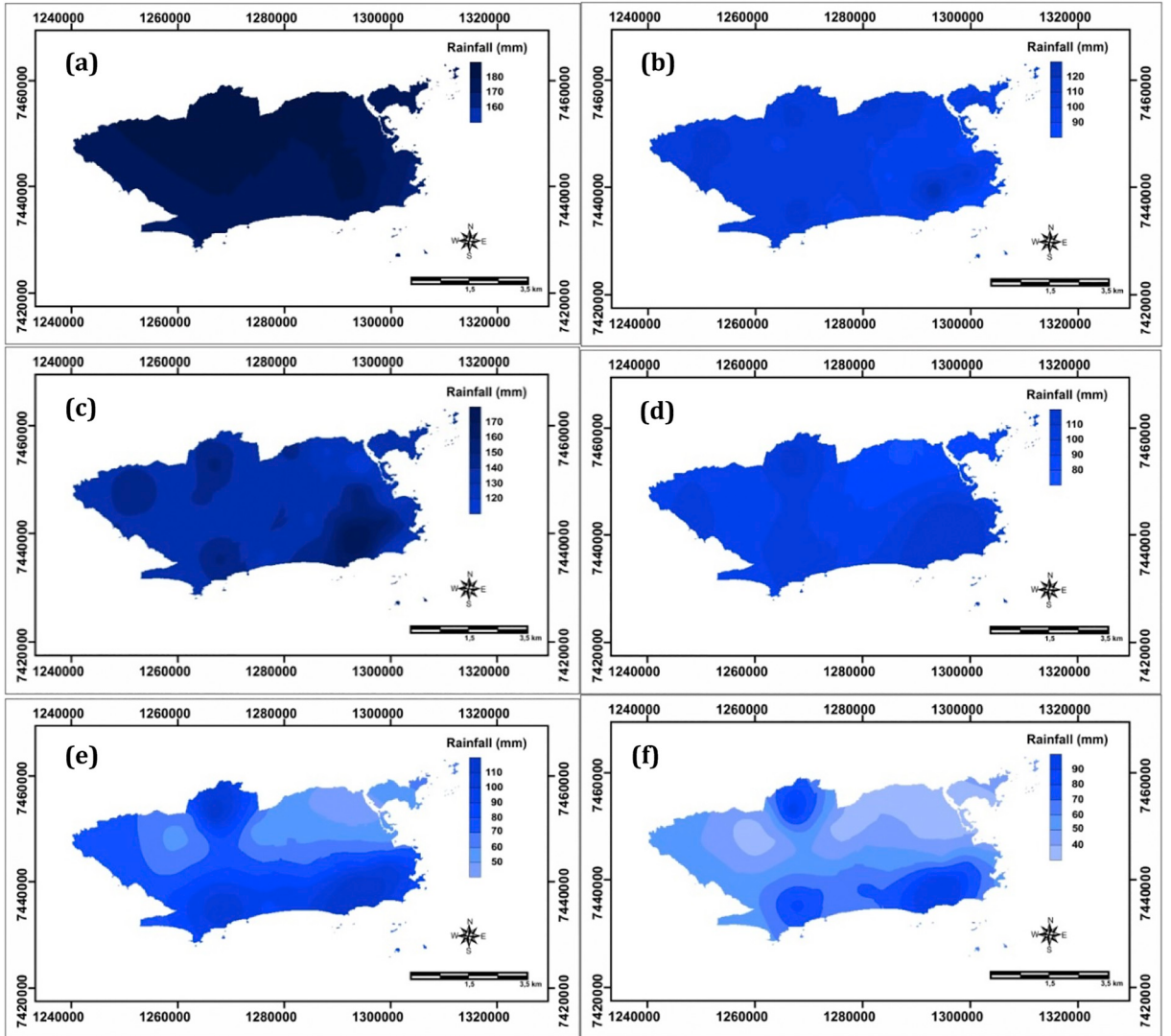


Fig. 4. Dendrogram (a) and number of groups (b) for rainfall in the municipality of Rio de Janeiro, Brazil.

$$d_E = \sqrt{\sum_{j=1}^p (x_{ij} - x_{kj})^2} \quad (9)$$

where d_E = Euclidian distance; x_{ij} and x_{kj} = quantitative variables j of individuals p and k, respectively.

In the Ward's method (1963) the distance between two clusters is the sum of the squares between them considering all variables. In this method, dissimilarity is minimized, or the total sum of squares within groups is minimized, that is, homogeneity within each group and heterogeneity outside each group is given (Lyra et al., 2014; Brito et al., 2016).

$$W = \sum_{i=1}^n x_i^2 - \frac{1}{n} (\sum x_i)^2 \quad (10)$$

where W = homogeneity and heterogeneity within groups by summing the square of the deviations; n = number of analysed values; x_i = i^{th} group element.

According to Kubrusly (2001), this method proves to be one of the most appropriate in clustering analysis. Rainfall data was organized as a matrix $P_{(n \times p)}$, where the element P_{ij} represents the value of the i^{th} variable (locality) of the j^{th} individual (month). Each vector line represents rainfall within the year and each vector column the different stations.

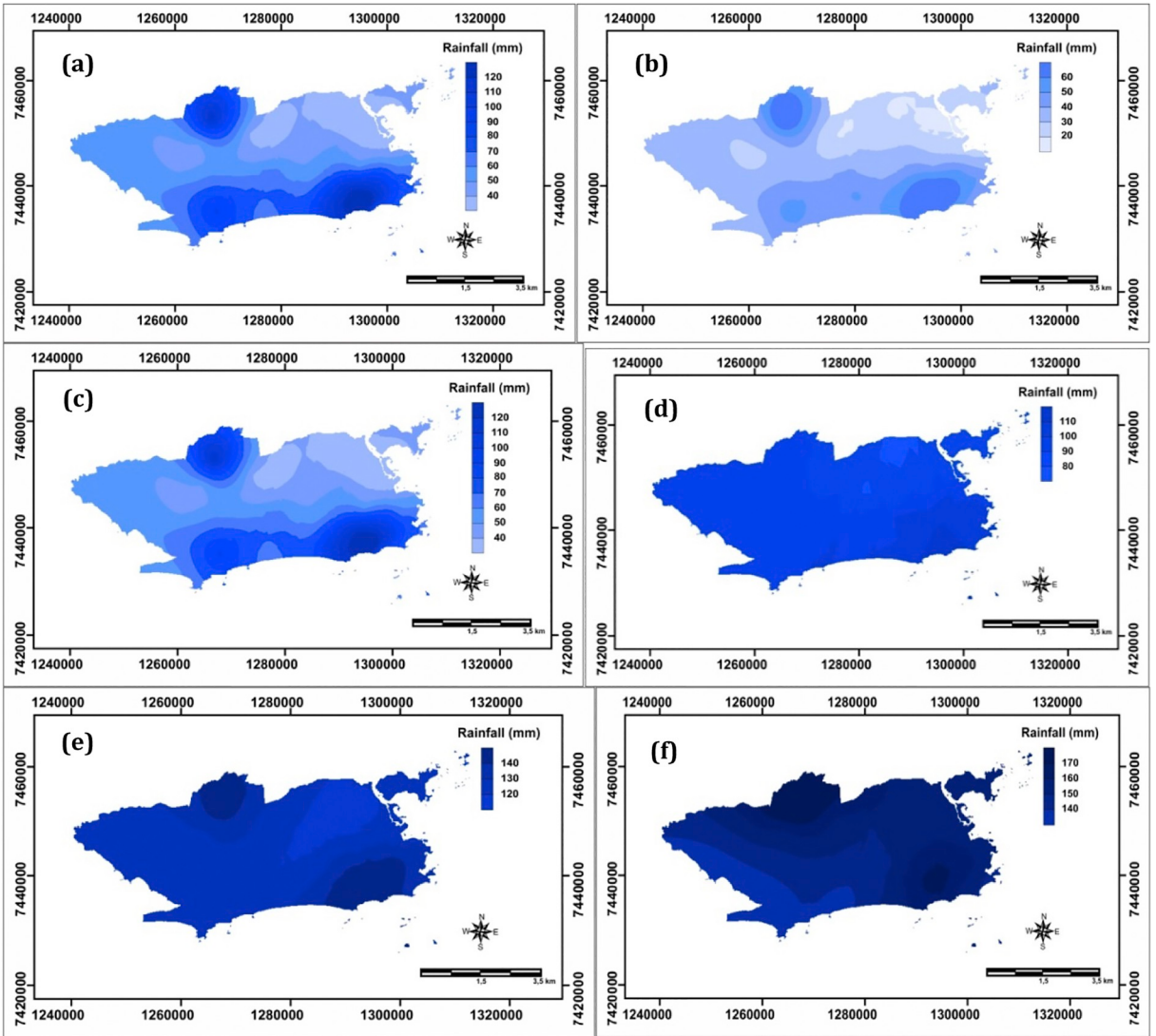


Fig. 5. Spatial distribution of homogeneous rainfall groups for the municipality of Rio de Janeiro.

2.6. Descriptive and exploratory analysis of rainfall data

The descriptive and exploratory analysis of the rainfall data were performed in the respective groups G_1 , G_2 , G_3 and G_4 , based on the cluster analysis (CA) and the parametric SW and B tests. The position and dispersion measurements are influenced by the presence of outliers. Applying descriptive statistics values for average, median, maximum, total amplitude, upper and lower limits, coefficients of variation (CV,%), asymmetry (Ap), kurtosis (K), standard deviation (SD), lower quartile (LQ), higher (HQ) and interquartile range (IQR) were calculated. This data statistic was determined using software R version 3.3.2 ([R Core Team, 2016](#)).

3. Results and discussion

3.1. Spatial rainfall pattern

3.1.1. Annual distribution

As in the studies of [Bernardes \(1953\)](#), [Brandão \(1987\)](#) and [Dereczynski et al. \(2009\)](#), the topography is an essential factor in the spatial distribution of rainfall in the MRJ, which presented an annual average of 1236 mm. The sectors located near the Gericino and Tijuca massifs presented the highest average annual rainfall records (> 1600 mm). Counterwise, the northern zone of the MRJ revealed drier characteristics, with rainfall totals lower than 1000 mm annually. It is precisely the region with the lowest altimetric elevations and located leeward of the coastal massifs of Tijuca and Pedra Branca. For the other areas, annual rainfall was predominant between 1000 mm and 1200 mm for the north central sector and above 1400 mm for the coastal south region, revealing the

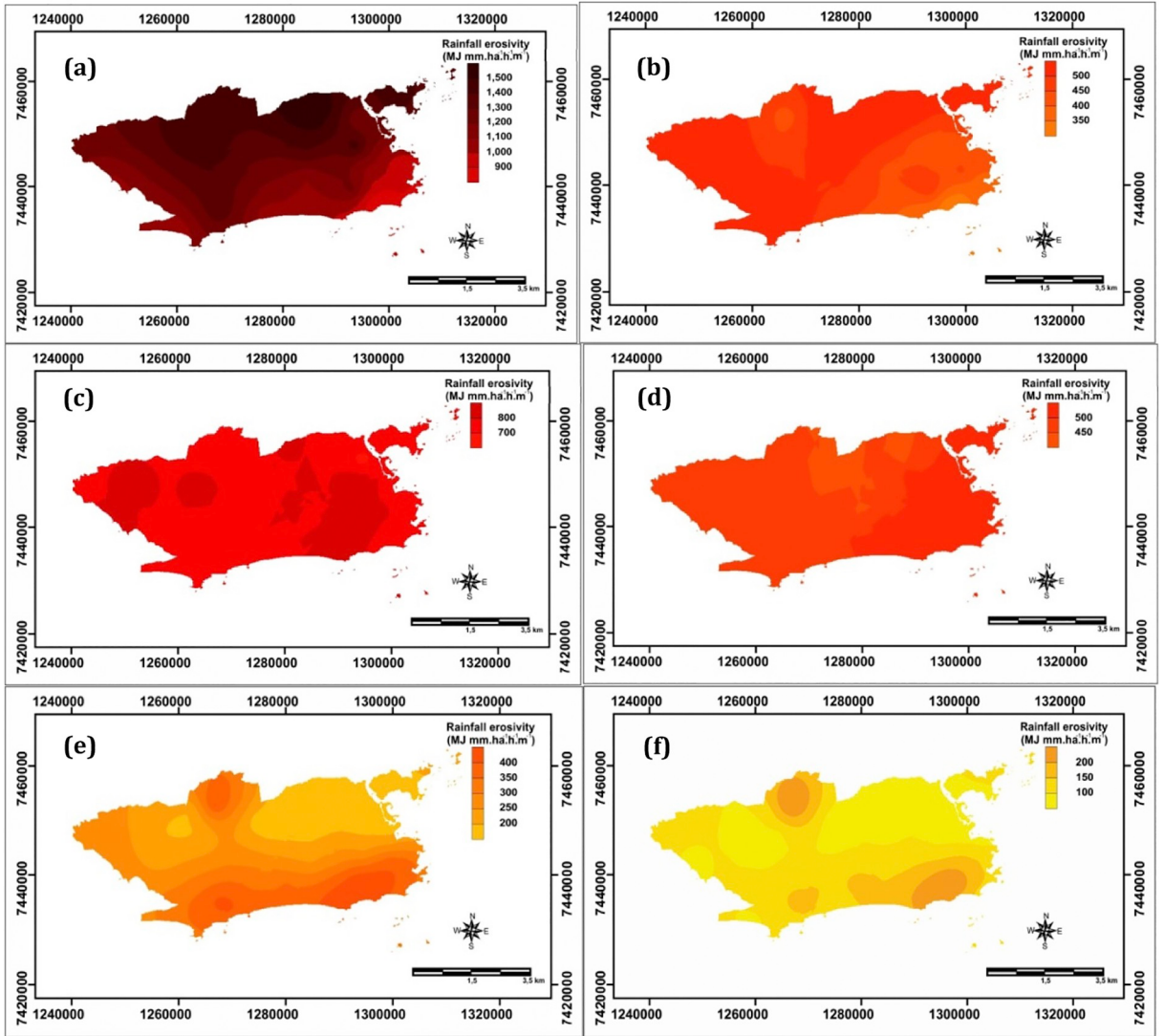


Fig. 6. Annual (a) and monthly (b) distribution of rainfall in the homogeneous groups of the municipality of Rio de Janeiro.

influence of the Atlantic Ocean on the spatial distribution of rainfall in the MRJ (Fig. 2).

Regarding rainfall climatology in the MRJ there are few references using long series of observational data. In addition, most references were developed in the 1950s and 1970s, according to Dereczynski et al. (2009). According to Serra and Ratisbonna (1957) and Serra (1970), annual rainfall totals increased from 1200 mm near the coast of the South Zone of the MRJ up to 1600 mm to the leeward region of the Tijuca massif.

3.1.2. Seasonal distribution

The presence of the Gericino - Mendenha, Tijuca and Pedra Branca massifs, in the Metropolitan Region of Rio de Janeiro (MRRJ), form physical barriers to the movement of air at lower levels of the atmosphere. This interaction results in changes of circulation patterns in local and adjacent weather conditions, together with the Bays of Sepetiba and Guanabara, which interfere in the rainfall regimes via bay, sea and land breezes (Moraes et al., 2005; Oliveira-Júnior et al., 2013).

The period between September and April (Fig. 3a-d and 3i-3l) accounts for 77.9% of annual average rainfall in the MRJ. The rainiest months of the historical series are January (175 mm) and December (157 mm), while June (59 mm) and August (42 mm) present the lowest average rainfall for the city. The pattern of monthly rainfall distribution follows, to a certain extent, the spatiality observed for the annual scale and, therefore, the highest totals are observed in the south, southeast and north regions of the MRJ. The lowest rainfall averages are registered in the northeast region, especially between March and November (Fig. 3c-3k). However, in the months of December (Fig. 3l) and January (Fig. 3a), the highest and lowest rainfall totals are registered in the north and west regions, respectively (Fig. 3).

In addition, present rainfall distribution in the MRJ is in agreement with the results of Keller Filho et al. (2005) for Brazil, and

Table 2

Descriptive statistics of monthly rainfall totals in groups (G1, G2, G3 and G4) in MRJ, Brazil.

Groups	Pluviometric stations	Average (mm)	Median (mm)	Values			Limits	
				Minimum (mm)	Maximum (mm)	Amplitude (mm)	Bottom (mm)	Higher (mm)
G1	Penha	75.56	57.20	1.00	374.40	373.40	-87.79	222.91
G1	Bangu	85.65	68.20	0.00	444.00	444.00	-73.33	227.68
G1	Piedade	89.93	74.70	1.80	347.20	345.40	-87.58	244.63
G1	Jacarepaguá/Tanque	90.23	71.60	1.80	435.00	433.20	-69.16	230.74
G1	Saúde	89.25	75.20	1.40	333.00	331.60	-84.90	244.70
G1	Jacarepaguá/Cidade de Deus	89.91	1.61	3.39	66.93	42.75	117.20	74.45
G1	Sepetiba	92.77	79.50	1.20	392.60	391.40	-92.98	265.63
G1	Gericinó	97.94	77.25	0.03	573.54	573.51	-95.22	268.89
G2	Vidigal	107.15	92.30	1.40	435.60	434.20	-79.86	282.64
G2	Jardim Botânico	119.20	100.90	3.00	521.00	518.00	-105.13	335.88
G2	Recreio dos Bandeirantes	92.54	77.85	0.80	465.80	465.00	-63.25	232.55
G2	Laranjeiras	108.81	93.17	2.20	403.60	401.40	-84.93	286.88
G3	Av. Brasil/Mendanha	153.11	117.90	0.20	610.00	609.80	-144.83	402.50
G4	Rocinha	140.53	121.75	1.80	571.00	569.20	-104.36	369.34
G4	Grota Funda	122.08	108.10	3.80	548.40	544.60	-90.00	307.20
G4	Mendanha	126.22	109.90	0.81	576.17	575.36	-100.62	338.51
Groups	Pluviometric stations	Coefficients	Asymmetry (Ap)	Curtosis (K)	Sample standard deviation (SD) (mm)	Quartile	Interquartile amplitude (mm)	
		Sample variance (%)			Bottom (mm)	Higher (mm)		
G1	Penha	85.33	1.56	2.98	64.47	28.73	106.40	77.68
G1	Bangu	80.71	1.77	4.65	69.12	39.55	114.80	75.25
G1	Piedade	77.63	1.28	1.66	69.82	37.00	120.05	83.05
G1	Jacarepaguá/Tanque	80.44	1.87	4.71	72.59	43.30	118.28	74.98
G1	Saúde	75.56	1.15	1.17	67.43	38.70	121.10	82.40
G1	Jacarepaguá/Cidade de Deus	74.45	1.61	3.39	66.93	42.75	117.20	74.45
G1	Sepetiba	75.37	1.19	1.80	69.92	41.50	131.15	89.65
G1	Gericinó	85.45	2.06	6.96	83.69	41.32	132.35	91.03
G2	Vidigal	67.66	1.25	2.36	72.50	56.08	146.70	90.63
G2	Jardim Botânico	66.91	1.32	2.85	79.75	60.25	170.50	110.25
G2	Recreio dos Bandeirantes	72.21	1.88	5.94	66.82	47.68	121.63	73.95
G2	Laranjeiras	68.72	1.06	1.17	74.77	54.50	147.45	92.95
G3	Av. Brasil/Mendanha	81.17	1.31	1.35	124.29	60.42	197.25	136.83
G4	Rocinha	67.19	1.19	1.85	94.42	73.28	191.70	118.43
G4	Grota Funda	68.82	1.45	3.30	84.02	58.95	158.25	99.30
G4	Mendanha	73.38	1.82	5.31	92.62	64.05	173.83	109.78

André et al. (2008), Brito et al. (2016) and Sobral et al. (2018) for the SRJ. These works indicate that the tropical climate proper to Central Brazil is characterized by the predominant rainfall concentration in the spring and summer period (September to March). Comparatively, the results of the pluviometric average obtained in this study are smaller than those observed by Sobral et al. (2018) for MRRJ, since these authors indicated averages greater than 200 mm for the months of January and December and approximately 60 mm for the months of June and August (Fig. 3f-3h).

The main meteorological systems that operate in the MRRJ range from synoptic to local scales and are rainfall producers or inhibitors. These main systems are Frontal Systems (FS), Mesoscale Convective Systems (MCS), South Atlantic Convergence Zone (SACZ), South Atlantic Subtropical High (SASH), Atmospheric Blocks (AB), different breeze systems (Satyamurty et al. 1998), orographic rainfall, convective storms, among others (Satyamurty et al., 1998; Dereczynski et al., 2009; Seluchi and Chou, 2009; Cataldi et al., 2010; Oliveira-Júnior et al., 2013; Oliveira-Júnior et al., 2014; Zandonadi et al., 2015; Oscar Júnior, 2018).

The main mechanisms of rainfall generation in the MRJ correspond to FS and the SACZ, especially during summer and spring seasons. The SACZ is an important phenomenon that favors episodes of floods and landslides, mainly in the MRRJ, being characterized by the passage of clouds in the Southeast-Northwest (SE-NW) direction, extending from the Amazon to the South Atlantic Ocean, associated to a humidity convergence zone that extends until the medium troposphere (Kousky, 1988; Carvalho et al., 2004; Quadro et al., 2012; Oliveira-Júnior et al., 2014).

The FS are associated with large-scale atmospheric flows, and the south and southeastern regions of Brazil are considered frontogenetic, where FS can form or intensify (Satyamurty and Mattos, 1989). As FS are active during all seasons, they are a

Table 3

Bartlett's parametric test on the monthly scale for the pluviometric stations – Significant (S) and Non-significant (NS).

ID	Pluviometric stations	Jan	Feb	Mar	Apr	May	Jun	Jul	Aug	Sep	Oct	Nov	Dec
1	Vidigal	S	S	S	S	S	S	S	S	S	S	S	S
2	Urca	S	S	S	S	S	S	S	S	S	S	S	S
3	Rocinha	S	S	S	S	S	S	S	S	S	S	S	S
4	Tijuca	S	S	S	S	S	S	S	S	S	S	S	S
5	Santa Teresa	S	S	S	S	S	S	S	S	S	S	S	S
6	Copacabana	S	S	S	S	S	S	S	S	S	S	S	S
7	Grajaú	S	S	S	S	S	S	S	S	S	S	S	S
8	Ilha do Governador	S	S	S	S	S	S	S	S	S	S	S	S
9	Penha	S	S	S	S	S	S	S	S	S	S	S	S
10	Madureira	S	S	S	S	S	S	S	S	S	S	S	S
11	Irajá	S	S	S	S	S	S	S	S	S	S	S	S
12	Bangu	S	S	S	S	S	S	S	S	S	S	S	S
13	Piedade	S	S	S	S	S	S	S	S	S	S	S	S
14	Jacarepaguá/Tanque	S	S	S	S	S	S	S	S	S	S	S	S
15	Saúde	S	S	S	S	S	S	S	S	S	S	S	S
16	Jardim Botânico	S	S	S	S	S	S	S	S	S	S	S	S
17	Barra/Barrinha	S	S	S	S	S	S	S	S	S	S	S	S
18	Jacarepaguá/Cidade de Deus	S	S	S	S	S	S	S	S	S	S	S	S
19	Barra/Riocentro	S	S	S	S	S	S	S	S	S	S	S	S
20	Guaratiba	S	S	S	S	S	S	S	S	S	S	S	S
21	Santa Cruz	S	S	S	S	S	S	S	S	S	S	S	S
22	Grande Méier	S	S	S	S	S	S	S	S	S	S	S	S
23	Anchieta	S	S	S	S	S	S	S	S	S	S	S	S
24	Grota Funda	S	S	S	S	S	S	S	S	S	S	S	S
25	Campo Grande	S	S	S	S	S	S	S	S	S	S	S	S
26	Sepetiba	S	S	S	S	S	S	S	S	S	S	S	S
27	Recreio dos Bandeirantes	S	S	S	S	S	S	S	S	S	S	S	S
28	Gericinó	S	S	S	S	S	S	S	S	S	S	S	S
29	Av. Brasil/Mendanha	S	S	S	S	S	S	S	S	S	S	S	S
30	Mendanha	S	S	S	S	S	S	S	S	S	S	S	S
31	Alto da Boa Vista	S	S	S	S	S	S	S	S	S	S	S	S
32	Laranjeiras	S	S	S	S	S	S	S	S	S	S	S	S
33	São Cristóvão	S	S	S	S	S	S	S	S	S	S	S	S

fundamental part of the rainfall regime in the MRJ and, moreover, interact more frequently in the rainy season with the convective systems, organizing and accentuating rainfall over the region.

3.1.3. Clustering and spatio-temporal patterns analyses for rainfall

Clustering technique results divided the MRJ in four homogeneous regions for rainfall characteristics, according to the cut-off point determined for dendograms for the identification of the ideal number of homogeneous groups (Fig. 4a and b). Homogeneous group I (HGI) presented 18 pluviometric stations, located in the central, western, north and northeast sectors. Homogeneous group II (HGII) is formed by 4 stations located in the south-central and south-east sectors, while HGIII is located at the extreme north (ID29) for rainfall. Homogeneous group IV (HGIV) is located to the north and southeast for rainfall (Fig. 5).

Results of grouping showed that the MRJ presents well defined spatial and temporal distribution of rainfall (Figs. 5 and 6). HGI is characterized by annual average rainfall of 1084.1 mm, attributed to lower altitudes and the location of the stations farthest from the shoreline. With an annual average of 1240.5 mm, HGII presents intermediary condition in relation to the other groups, also with lower altitudes. However, HGII is composed of stations closer to the Atlantic Ocean, which helps to explain greater values of rainfall when compared to HGI. In an anomalous condition, HGIII is characterized by the greatest annual rainfall of MRJ, even at lower altitudes in relation to HGIV, registering annually an average of 1837.4 mm (Fig. 6a). On the other hand, HGIV is located in conditions of higher altitudes in different sectors of the MRJ, registering an annual rainfall total of 1584.5 mm.

It was perceived the influence of the orography in the spatial distribution of the annual rainfall for the MRJ, although it is not a mandatory condition, since the rainier sector of the city does not occur necessarily on the highest elevation stations. This occurs because stations with lower altitudes in HGIII are located in areas of abrupt transition from the coast to the coastal massif. In these areas, although the stations are often at lower altitudes, the interaction between humidity and the litoral massifs causes atmospheric instability, resulting in rainfall. Particularly, HGIII is located in one of the most intense sectors of heat islands, identified by Brandão (1996). HGIII stations are also located near an urban expansion area invigorated by Avenida Brasil avenue, an aspect responsible for increasing convective activity and rainfall generation.

As for annual variability (Fig. 6a), values lower than 1000 mm for HGI and HGII were often registered, with HGI (698 mm) being the most prominent in 2014. Even so, HGI is the driest group for MRJ (847 mm), apparently not influenced by surface temperature anomalies of the Pacific Ocean (NOAA, 2018). The highest annual rainfall for the whole series was registered by HGIII during 2005 (3105 mm), 2006 (3440 mm) and 2009 (3188 mm), years of low to moderate El Niño conditions (Grimm and Tedeschi, 2009; Terassi et al., 2018; Sobral et al., 2018). Results showed that local rainfall conditions, such as orography and local convection (Dereczynski

Table 4

Shapiro-Wilk's parametric test on the monthly scale for the pluviometric stations – Significant (S) and Non-significant (NS).

ID	Pluviometric stations	Jan	Feb	Mar	Apr	May	Jun	Jul	Aug	Sep	Oct	Nov	Dec
1	Vidigal	NS	NS	NS	S	NS	NS	S	S	NS	NS	NS	NS
2	Urca	NS	S	NS	S	NS	NS	S	NS	S	S	NS	NS
3	Rocinha	S	NS	NS	S	NS	S	S	S	NS	NS	NS	NS
4	Tijuca	NS	S	NS	S	S	NS	NS	S	S	S	NS	NS
5	Santa Teresa	NS	S	NS	S	S	NS	NS	S	NS	S	NS	NS
6	Copacabana	S	NS	S	S	NS	S	NS	S	NS	NS	NS	S
7	Grajaú	NS	NS	NS	S	NS	NS	NS	S	NS	S	NS	NS
8	Ilha do Governador	NS	NS	S	S	NS	NS	NS	S	NS	NS	NS	S
9	Penha	NS	NS	NS	S	NS	NS	NS	S	NS	S	NS	S
10	Madureira	NS	NS	S	S	NS	NS	S	NS	NS	NS	NS	S
11	Irajá	NS	NS	NS	S	NS	NS	S	S	NS	NS	NS	S
12	Bangu	S	NS	NS	S	NS	S						
13	Piedade	NS	NS	NS	S	S	NS	NS	S	NS	NS	NS	NS
14	Jacarepaguá/Tanque	NS	NS	S	S	NS	NS	NS	S	NS	NS	NS	S
15	Saúde	NS	NS	NS	S	NS	NS	S	S	NS	NS	NS	NS
16	Jardim Botânico	NS	NS	NS	S	NS	NS	S	S	NS	NS	NS	NS
17	Barra/Barrinha	S	S	S	S	S	S	S	NS	NS	NS	NS	S
18	Jacarepaguá/Cidade de Deus	NS	NS	S	S	NS	NS	NS	S	NS	NS	NS	S
19	Barra/Riocentro	S	NS	S	S	NS	S	NS	S	S	S	NS	S
20	Guaratiba	NS	NS	NS	S	S	NS	S	S	S	S	NS	S
21	Santa Cruz	S	NS	NS	NS	NS	NS	NS	S	NS	NS	NS	NS
22	Grande Méier	NS	NS	S	S	NS	NS	NS	S	NS	NS	NS	S
23	Anchieta	NS	NS	S	S	NS	NS	NS	S	NS	NS	NS	S
24	Grota Funda	NS	NS	NS	S	NS	NS	NS	S	S	S	NS	NS
25	Campo Grande	S	NS	NS	S	NS	NS	NS	S	NS	S	NS	S
26	Sepetiba	NS	NS	S	NS	S	NS	NS	S	NS	S	NS	S
27	Recreio dos Bandeirantes	S	NS	S	S	NS	NS	NS	S	NS	S	NS	S
28	Gericinó	S	NS	NS	S	NS	S	S	NS	NS	NS	NS	S
29	Av. Brasil/Mendanha	NS	NS	NS	S	NS	S	S	NS	NS	NS	NS	S
30	Mendanha	NS	NS	S	S	NS	NS	S	S	NS	NS	NS	NS
31	Alto da Boa Vista	S	S	S	S	S	S	S	NS	NS	NS	NS	S
32	Laranjeiras	NS	NS	NS	S	NS	NS	NS	S	S	NS	S	NS
33	São Cristóvão	NS	NS	NS	S	NS	NS	NS	S	NS	S	NS	S

et al., 2009; Zeri et al., 2011), allow the occurrence of annual differences greater than 2300 mm between HGII and HGIII, being verified in the year of 2006 (Fig. 6a).

The MRJ sector which registered lower rainfall totals in the monthly scale is HGII, with values lower than 50 mm in June, July and August, when the average accumulated rainfall is 119.3 mm. During the same trimester, HGIII and HGIV register averages of 290.3 and 256.1 mm. The rainiest three months for the study area occur in January, March and December for HGII, HGIII and HGIV, with average rainfall totals above 130 mm. Differently, HGIII is characterized by highest values of rainfall (> 200 mm) in January, November and December. Therefore, during the rainier three months in HGIII an average of 680 mm of rainfall occurs, while in HGII the accumulated rainfall is 433 mm (Fig. 6b). This pattern of spatial-temporal distribution of monthly rainfall for MRJ was previously observed by Dereczynski et al. (2009), which observed the highest pluviometric totals in areas near the Tijuca (in the south), Gericino-Mendanha (in the north) and Pedra Branca (south-south) massifs. It is noteworthy that previous studies did not apply multivariate analysis and that stations of HGIII and HGIV in which approximately GHIII and GHIV are located in this area study.

It was perceived that even during the rainy season, in the period from September to March, the month of February presented a reduction of rainfall, also verified in the SRJ (Brito et al., 2016; Sobral et al., 2018). During Febrary, studies by Cupolillo et al. (2008) and Cupolillo (2015) attribute the frequent synoptic situation to the anomalous position of the Bolivian Highlands (BH), which favors the further south the occurrence of the Northeast Cavado, and consequently the formation of AB and a strong subsidence. This synoptic condition causes the reduction of rainfall even in HGIII (115 mm), which shows how large scale aspects interfere in the temporal distribution of rainfall in the MRJ.

3.1.4. Descriptive statistics and parametric tests applied to the pluviometric series

The descriptive statistics of the pluviometric time series revealed that groups of higher rainfall totals (HGIII and HGIV) present the highest values of averages, medians, amplitudes, standard deviation, limits of the quartiles (lower and upper), which demonstrates the pluvial abundance in these sectors of MRJ. Conversely, HGII and HGIII registered the lowest values for these statistical parameters, which corroborates with these sectors presenting the lowest rainfall totals in MRJ (Table 2).

The highest values of asymmetry (> 1.77) and kurtosis (> 4) were obtained for HGII (ID12 and 14), HGIII (ID28 and 27) and HGIV (ID30), indicating that these are the stations with greater rainfall variability. However, the sample variance was higher than 75%, predominantly for HGII and HGIII, with HGIII presenting the highest interquartile amplitude. These statistical parameters establish that the HGII and HGIII are the sectors with the highest rainfall variability, with the first group being characterized by minimum values of the quantal classes and HGIII presenting the maximum values established by the descriptive statistics (Table 2).

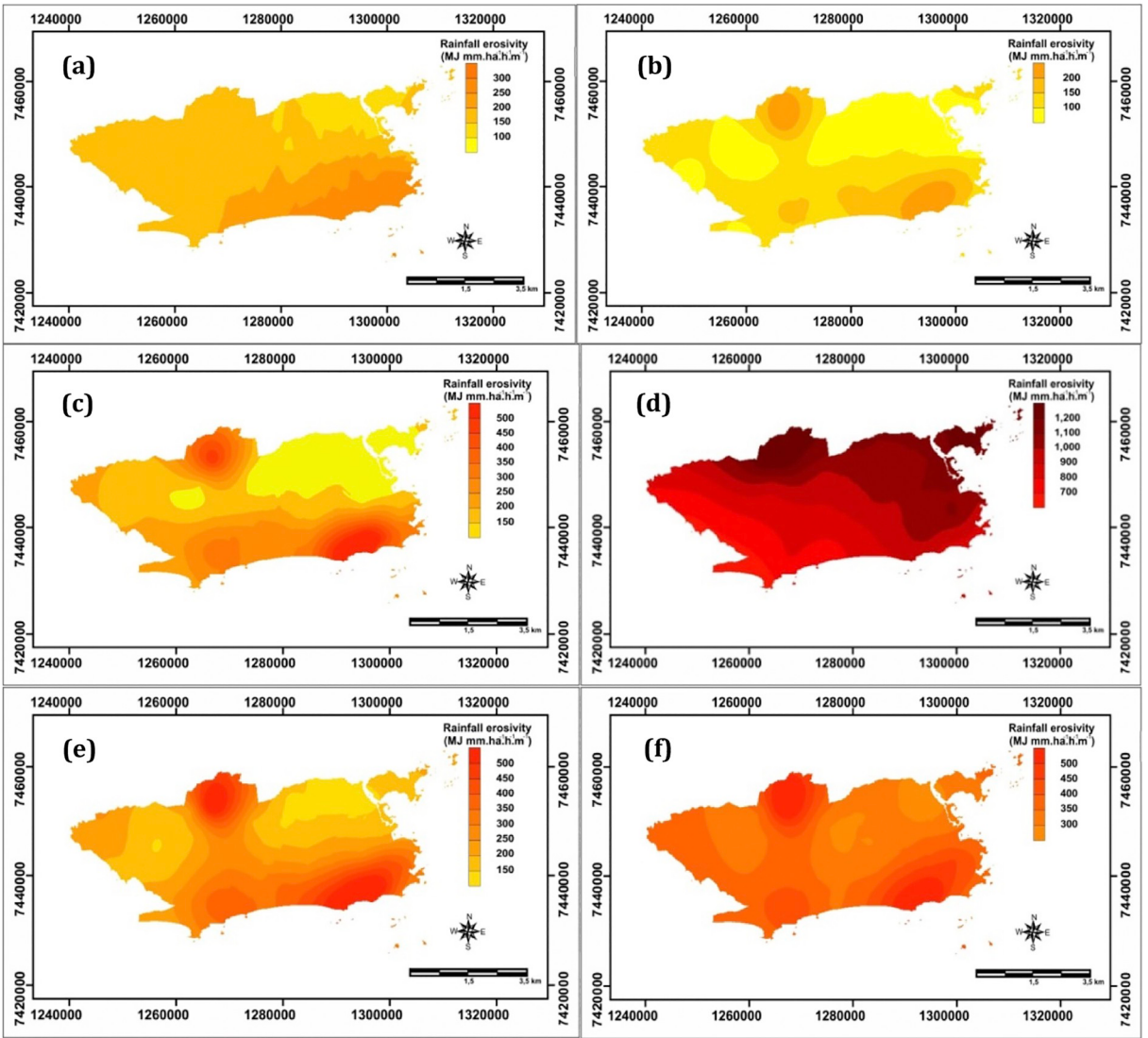


Fig. 7. Spatial distribution of the erosivity estimates (a) in the annual scale for the municipality of Rio de Janeiro, Brazil.

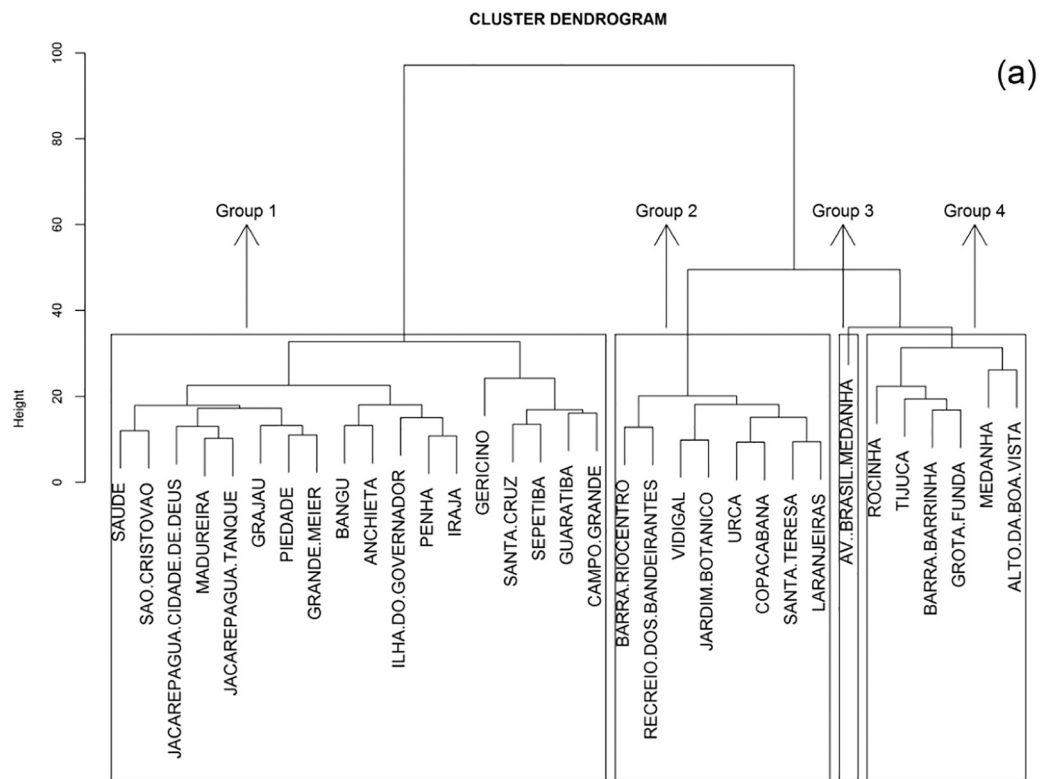
The application of the Bartlett (B) and Shapiro-Wilk (SW) tests made it possible to evaluate the homogeneity of variance and normality for rainfall data on the monthly scale. The B test revealed that homogeneity of variance is significant (S) for all pluviometric stations during all months, indicating that all time series are within the thresholds of variance (Table 3). (See Table 4.)

However, the SW test proved to be more effective in distinguishing non-significant (NS) and significant (S) data in the different pluviometric stations. Months of November (31 estações ou 94%) and February (28 estações ou 85%) registered the highest number of rainfall stations with non-significant (NS) series according to the SW test. That is most likely due to the climatic characteristics e da distribuição das chuvas nessas estações, both months of transition between seasons, with dry spells occurring in February (Cupolillo et al., 2008; Brito et al., 2016). It was observed that the months of April and August were more representative considering normality of data, in 31 and 28 of the 33 stations analyzed, in this order. That is attributed to the lower monthly rainfall variability in these periods, which depend on the passage of FS as the most active mechanism in rainfall generation, according to Armond and Sant'anna Neto (2017).

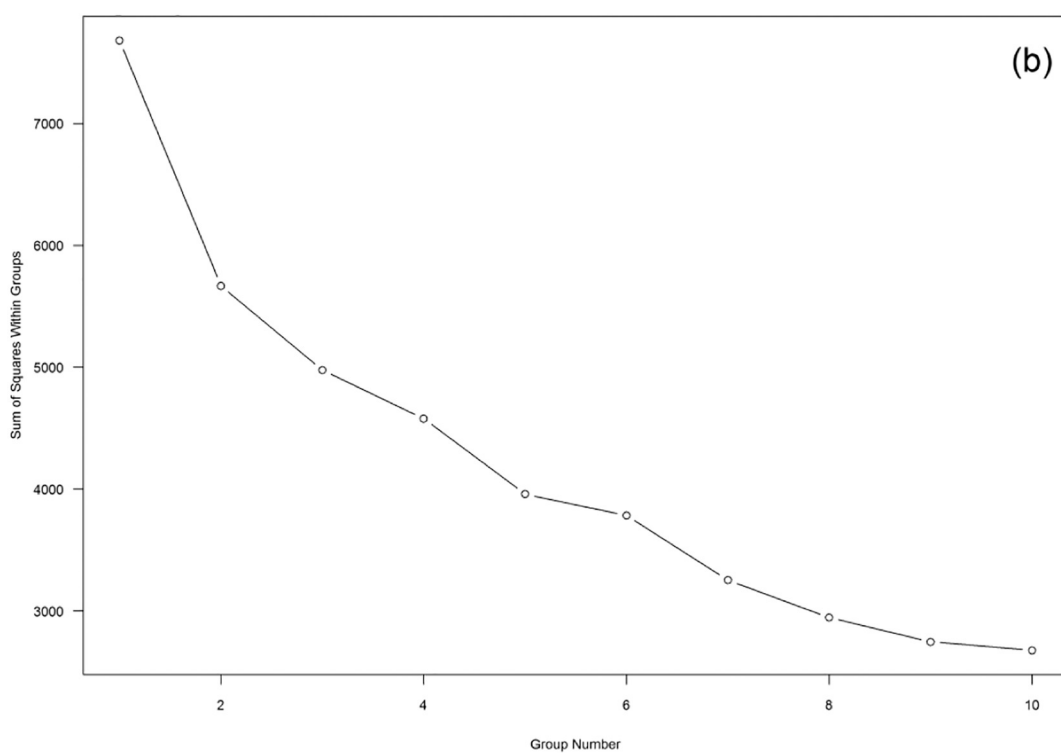
3.2. Spatial erosivity estimation pattern

3.2.1. Annual distribution

The spatial distribution of the erosion results for the MRJ indicated that the highest indices coincide with rainfall potential. Annual erosivity superior to $7000 \text{ MJ.mm.ha}^{-1} \cdot \text{h}^{-1} \cdot \text{year}^{-1}$ are registered in areas near the previously referenced massifs. Conversely, areas to the northeast and west of the MRJ register the lowest values of erosivity, below $5750 \text{ MJ.mm.ha}^{-1} \cdot \text{h}^{-1} \cdot \text{year}^{-1}$,



d
hclust (*, "ward.D")



(caption on next page)

Fig. 8. Spatial distribution of the erosivity estimates in the months of January (a), February (b), March (c), April (d), May (e), June (f), July (g), August (h), September (i), October (j), November (k) and December (l) in the municipality of Rio de Janeiro, Brazil.

in lower altitude areas. Erosivity potential registered an annual average of $6201 \text{ MJ.mm.ha}^{-1}.\text{h}^{-1}.\text{year}^{-1}$ (Fig. 7).

Erosivity index values are lower than those found for other regions of Brazil, such as the coasts of São Paulo (Sant'Anna Neto, 1995) and Paraná (Waltrick et al., 2015) states, with values greater than $10,000 \text{ MJ.mm.ha}^{-1}.\text{h}^{-1}.\text{year}^{-1}$. In Santa Catarina, Back et al. (2018) verified total annual erosivity greater than $11,000 \text{ MJ.mm.ha}^{-1}.\text{h}^{-1}.\text{year}^{-1}$ for the north coast and less than $5000 \text{ MJ.mm.ha}^{-1}.\text{h}^{-1}.\text{year}^{-1}$ in the south coast. However, they are consistent with the results obtained by Mello et al. (2012) to the southern coast of Espírito Santo state, which were predominant between 4000 and $6000 \text{ MJ.mm.ha}^{-1}.\text{h}^{-1}.\text{year}^{-1}$. The results for the municipality of Rio de Janeiro are similar to those verified by Mello et al. (2007) for the South of Minas Gerais, which showed an annual average between 4905 and $7357 \text{ MJ.mm.ha}^{-1}.\text{h}^{-1}.\text{year}^{-1}$.

3.2.2. Seasonal distribution

It was confirmed that months of January and December are the months of greater risks due to rainfall erosivity (Fig. 8). The month of January registered an average of $1185 \text{ MJ.mm.ha}^{-1}.\text{h}^{-1}.\text{month}^{-1}$, with higher values in the north region ($> 1500 \text{ MJ.mm.ha}^{-1}.\text{h}^{-1}.\text{month}^{-1}$) and lower values in the extreme southeast ($< 900 \text{ MJ.mm.ha}^{-1}.\text{h}^{-1}.\text{month}^{-1}$). During December, the erosivity is usually concentrated in the northern sector and *Ilha do Governador* district ($> 1200 \text{ MJ.mm}^{-1}.\text{ha}^{-1}.\text{h}^{-1}.\text{month}^{-1}$) and the lowest values are registered west ($< 700 \text{ MJ.mm.ha}^{-1}.\text{h}^{-1}.\text{month}^{-1}$) of the city. Another month of greater caution considering erosivity is March, which registered an average of $787 \text{ MJ.mm.ha}^{-1}.\text{h}^{-1}.\text{month}^{-1}$, with the spatial predominance of erosive potential between 700 and $800 \text{ MJ.mm.ha}^{-1}.\text{h}^{-1}.\text{month}^{-1}$ in the MRJ (Fig. 8c).

It was verified a concentration of 85.7% of the erosive potential between September and April, when the average erosivity of the MRJ is higher than $300 \text{ MJ.mm.ha}^{-1}.\text{h}^{-1}.\text{month}^{-1}$. During autumn and winter months (May – August) the average erosivity of the city does not reach the aforementioned threshold. August is the month that registered least susceptibility to the erosive factor ($133 \text{ MJ.mm.ha}^{-1}.\text{h}^{-1}.\text{month}^{-1}$), with values lower than $100 \text{ MJ.mm.ha}^{-1}.\text{h}^{-1}.\text{month}^{-1}$ at *Ilha do Governador* district, northeast and west regions (Fig. 8h).

These results indicate that the concentration of rainfall erosivity between spring and summer seasons is dominant in the Brazilian territory. Similar work by Almeida et al. (2012) observed that 94% of the annual erosion potential is concentrated between September and March for the state of Mato Grosso. The studies by Silva et al. (2010) for the Vale do Rio Doce region, in the eastern part of Minas Gerais state, indicate that 83% of annual erosivity occurs in the period between November and March. Due to the dominance of the subtropical climate and the frequent performance of FS throughout the year (Reboita et al., 2010; Borsato and Mendonça, 2015), there is a lower concentration of rainfall in the southern (Climate type "Cfa" and "Cfb") region of Brazil during summer, when compared to tropical climate regions of the country and, consequently, published literature indicates lower percentages of erosive potential for the rainy season in south Brazil. Schick et al. (2014) indicated that in Lages, located in the state of Santa Catarina, about 65% of annual average erosivity occurs between September and February, while in Rio Grande, further south in Rio Grande do Sul state, Bazzano et al. (2010) inferred that 57.9% of erosivity occurs in the same period.

3.2.3. Clustering and spatio-temporal patterns analyses for erosivity

Cluster analysis results indicate that erosivity and rainfall points present similarity, with the MRJ being subdivided into four homogeneous regions, according to the cut-off point determined for dendograms for the identification of the ideal number of homogeneous groups (Fig. 9a and b). Homogeneous group I (HGI) presented 18 pluviometric stations, located in the central, western, north and northeast sectors. Homogeneous group II (HGII) is formed by 4 stations located in the south-central and south-east sectors, while HGIII is located at the extreme north (ID29) and southeast (ID3 and 17) for erosivity. Homogeneous group IV (HGIV) is located to the north and southeast for erosivity (Fig. 10).

The grouping of pluviometric stations with similarity to erosivity showed that HGIII and HGIV are the sectors with the highest risks due to rainfall erosive potential, being characterized by an average annual erosivity of 7926.6 and $7513.9 \text{ MJ.mm.ha}^{-1}.\text{h}^{-1}.\text{year}^{-1}$. Opposingly, the lowest erosivity potential related to rainfall in MRJ occurred in HGI and HGII, in which the annual average was equivalent to 5750.1 and $6019.5 \text{ MJ.mm.ha}^{-1}.\text{h}^{-1}.\text{year}^{-1}$, in this order (Fig. 11a).

Therefore, the erosivity classified as high and very high, according to the classification of Foster et al. (1981), occurs in the higher sectors of the city and in the vicinity of the Gericino-Mendanha, Pedra Branca and Tijuca massifs. In these areas, local factors such as greater slope and shallow soils interact with more voluminous and erosive rainfall. It should be noted that residential occupation in these sectors of MRJ interfere directly in the hydrological dynamics of the slope, increasing the succession of mass movements Schlee et al. (2012).

The highest values of erosivity estimates in the MRJ were recorded in the HGIV during 2013 ($11,730.9 \text{ MJ.mm.ha}^{-1}.\text{h}^{-1}.\text{year}^{-1}$) and in the HGIII during 2003 ($11,368.6 \text{ MJ.mm.ha}^{-1}.\text{h}^{-1}.\text{year}^{-1}$), years of neutrality of ENSO anomalies. For HG I and II, the highest annual erosivity estimate occurred in 2010, with the values of 8635.7 and $9549.3 \text{ MJ.mm.ha}^{-1}.\text{h}^{-1}.\text{year}^{-1}$, in a period alternating between the El Niño and La Niña phases (NOAA 2018; Sobral et al., 2018). In the condition of neutrality of this anomaly, the year 2014 stands out due to the lower erosivity in the MRJ, with values lower than $4000 \text{ MJ.mm.ha}^{-1}.\text{h}^{-1}.\text{year}^{-1}$ for the HG I and II and equivalent to 5013 , $4 \text{ MJ.mm.ha}^{-1}.\text{h}^{-1}.\text{year}^{-1}$ for HGIII. The lowest annual erosivity for HGIV occurred in 1997 ($5080.8 \text{ MJ.mm.ha}^{-1}.\text{h}^{-1}.\text{year}^{-1}$) under El Niño conditions (Fig. 11a).

Monthly analysis of erosivity distribution in different homogeneous groups of MRJ establishes spatio-temporal patterns of erosion.

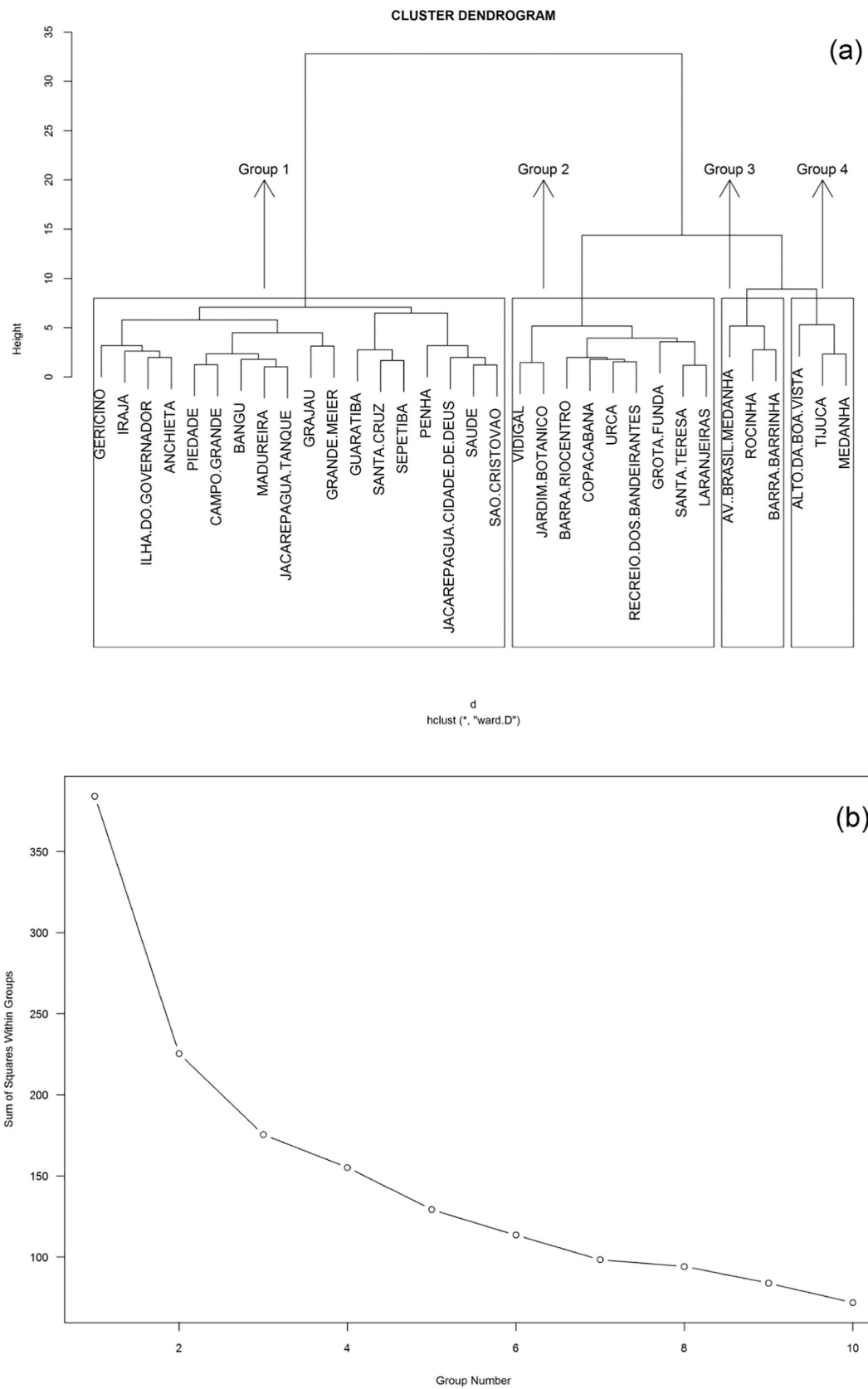


Fig. 9. Dendrogram (a) and number of groups (b) of the erosivity estimates in the municipality of Rio de Janeiro, Brazil.

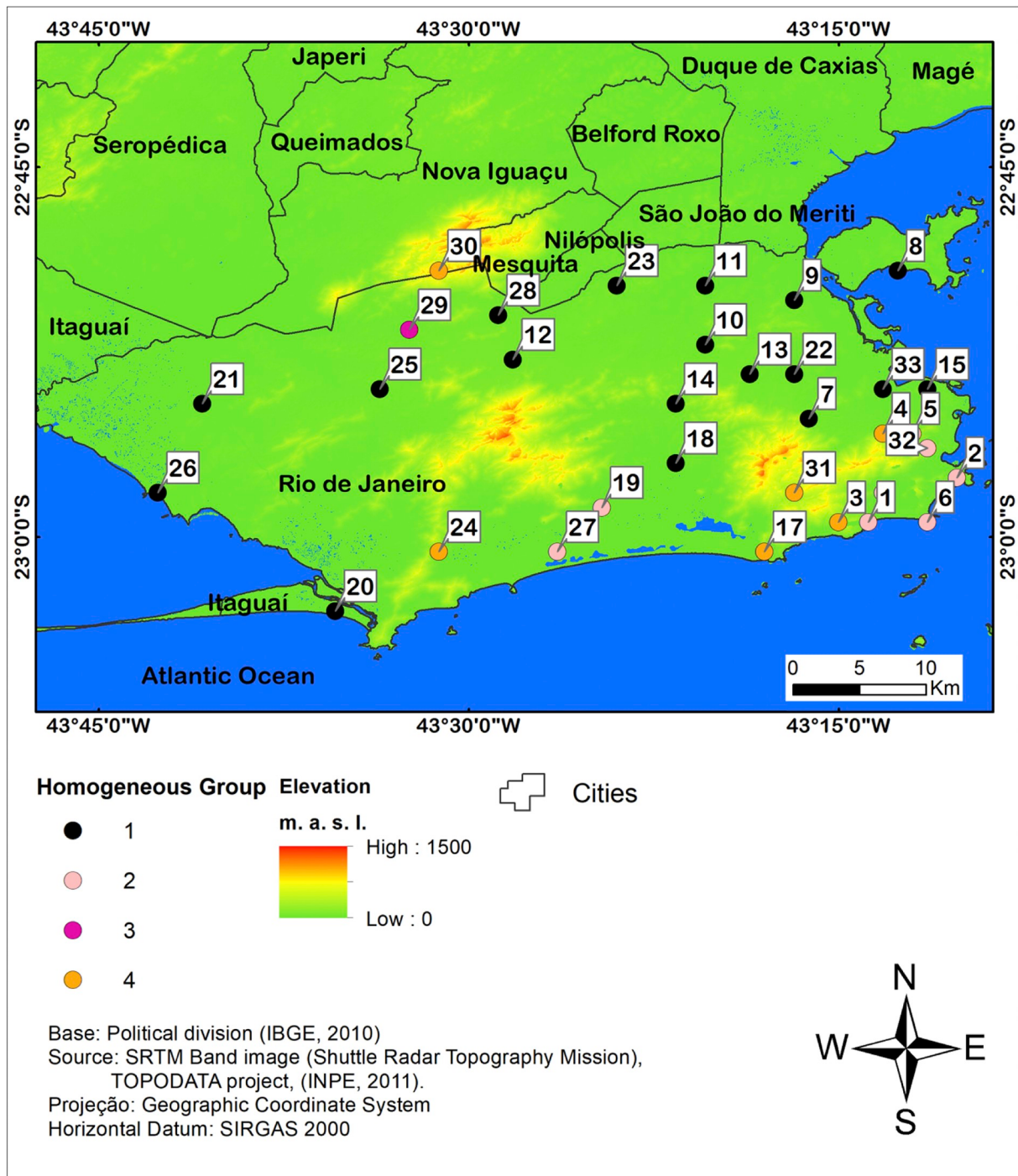


Fig. 10. Spatial distribution of homogeneous of the erosivity estimates of groups for the municipality of Rio de Janeiro.

HGI corresponds to the sector of lower estimates of erosivity in the period between April and November (autumn-spring), with values higher than $800 \text{ MJ.mm.h}^{-1}.\text{month}^{-1}$ only in January, March and December. Nevertheless, it is the sector with the highest monthly maximum value, registered in January ($1298.5 \text{ MJ.mm.h}^{-1}.\text{month}^{-1}$). HGII registered erosivity values higher than $600 \text{ MJ.mm.h}^{-1}.\text{month}^{-1}$ between November and January and in March, with a maximum erosivity in January ($990.8 \text{ MJ.mm.h}^{-1}.\text{month}^{-1}$). Although GHI is the sector of lower annual rainfall, GHII is less susceptible to monthly maximum erosivity values, since rainfall in this second group occurs less concentrated than in the first group (Fig. 11b).

It was noted that HGIII presents the highest values of erosivity ($> 1000 \text{ MJ.mm.h}^{-1}.\text{month}^{-1}$) between November and January and higher than $600 \text{ MJ.mm.h}^{-1}.\text{month}^{-1}$ during March, April, September and October. These months are the

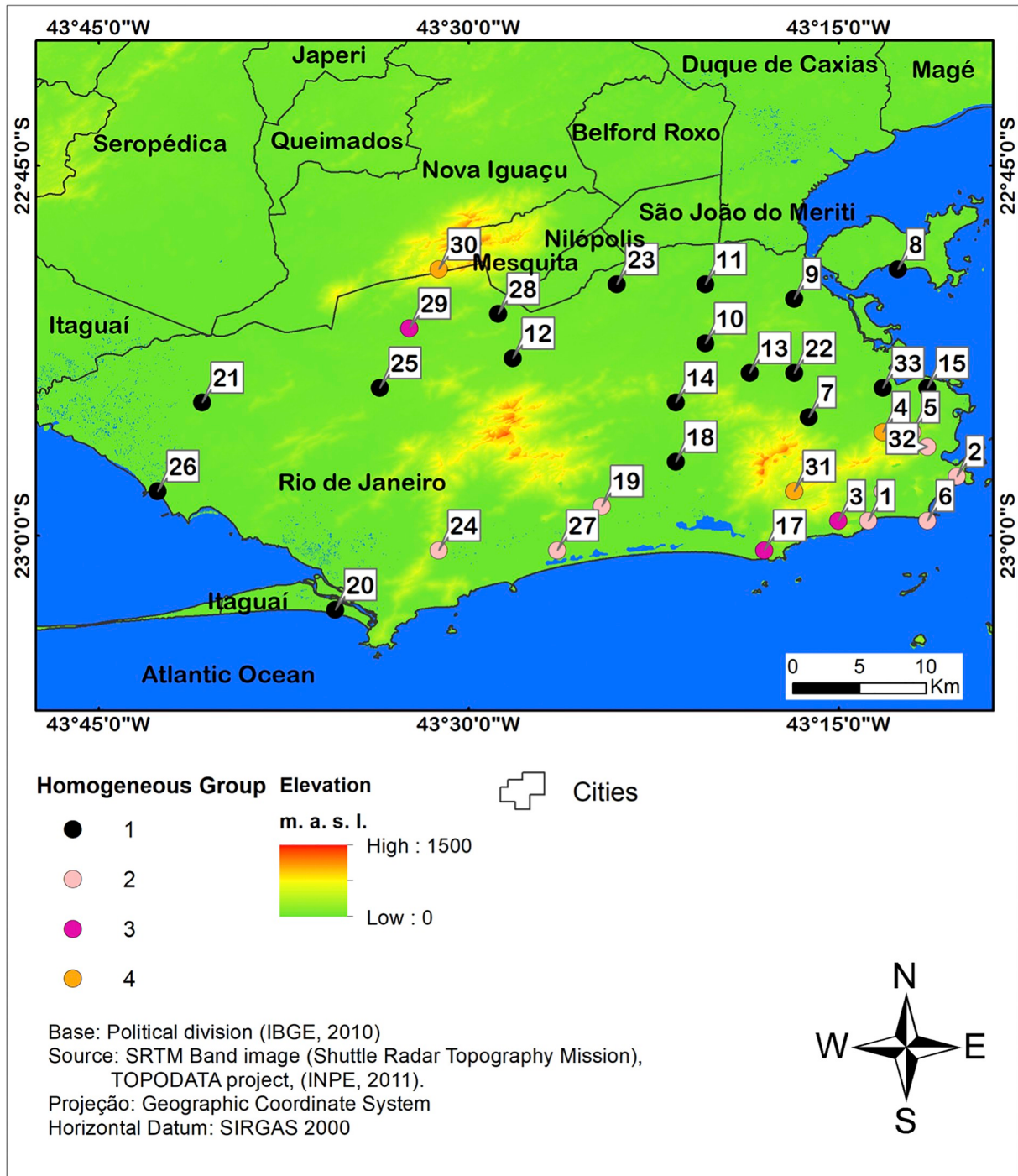


Fig. 11. Annual (a) and monthly (b) distribution of the erosivity estimates in the homogeneous groups of the municipality of Rio de Janeiro.

delimiters of the end and beginning of the rainy season in the SRJ (Sobral et al., 2018). It was also observed that HGIII expresses with greater intensity the occurrence of rainfall reduction in the month of February, registering the lowest erosive potential among all homogeneous groups for this month. On the other hand, HGIV is characterized by values greater than $750 \text{ MJ.mm.h}^{-1} \cdot \text{month}^{-1}$ between November and January; while in March and April, notably above $1000 \text{ MJ.mm.h}^{-1} \cdot \text{month}^{-1}$ in January and December (Fig. 11b).

HGIV registered the highest accumulated erosivity values in the months between November and April, equivalent to $5435 \text{ MJ.mm.h}^{-1} \cdot \text{month}^{-1}$, in relation to the same period in HGIII ($4953 \text{ MJ.mm.h}^{-1} \cdot \text{month}^{-1}$). However, it

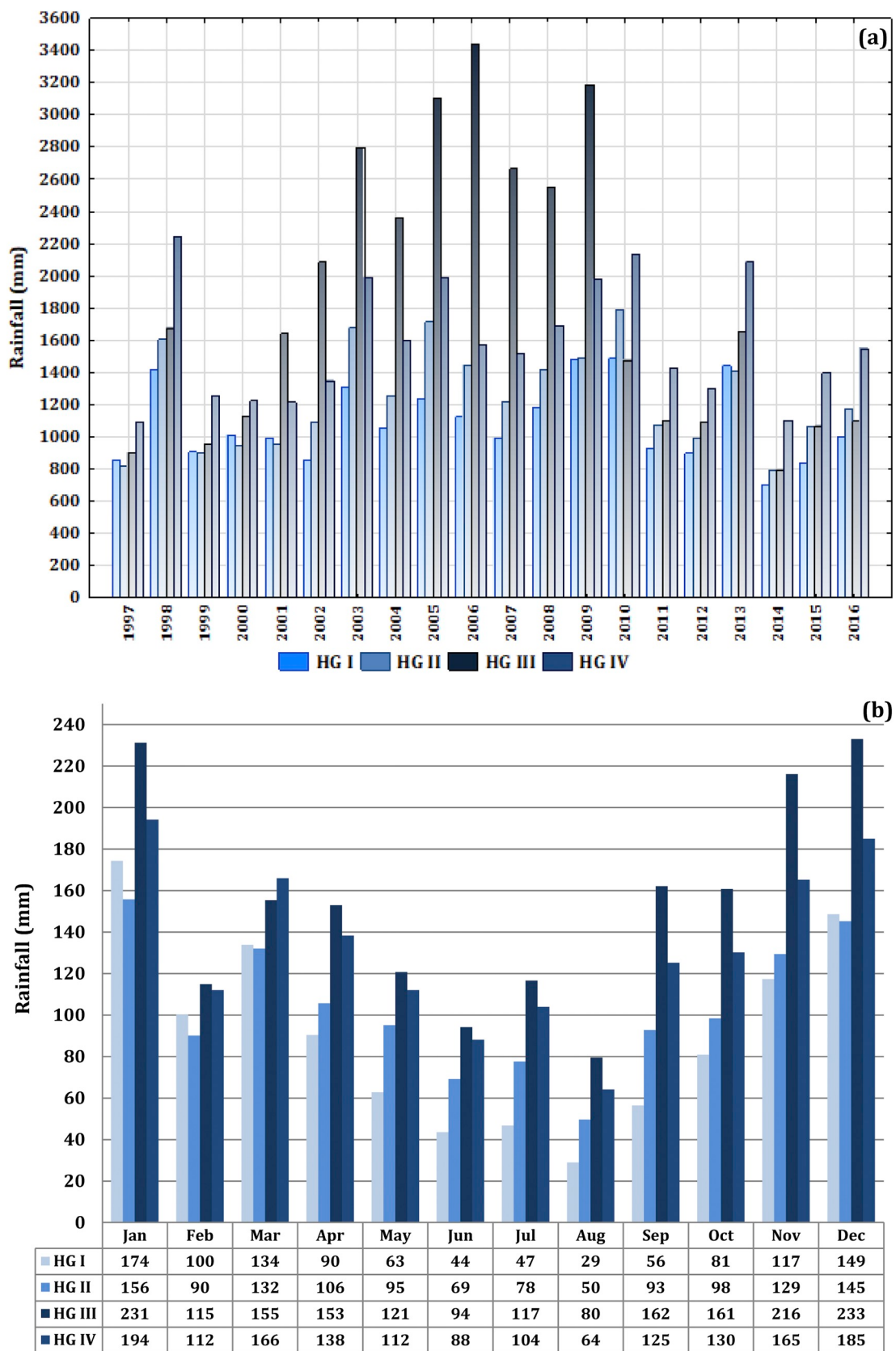


Fig. 12. Annual (a) and monthly (b) distribution of rainfall in the homogeneous groups of the city of Rio de Janeiro.

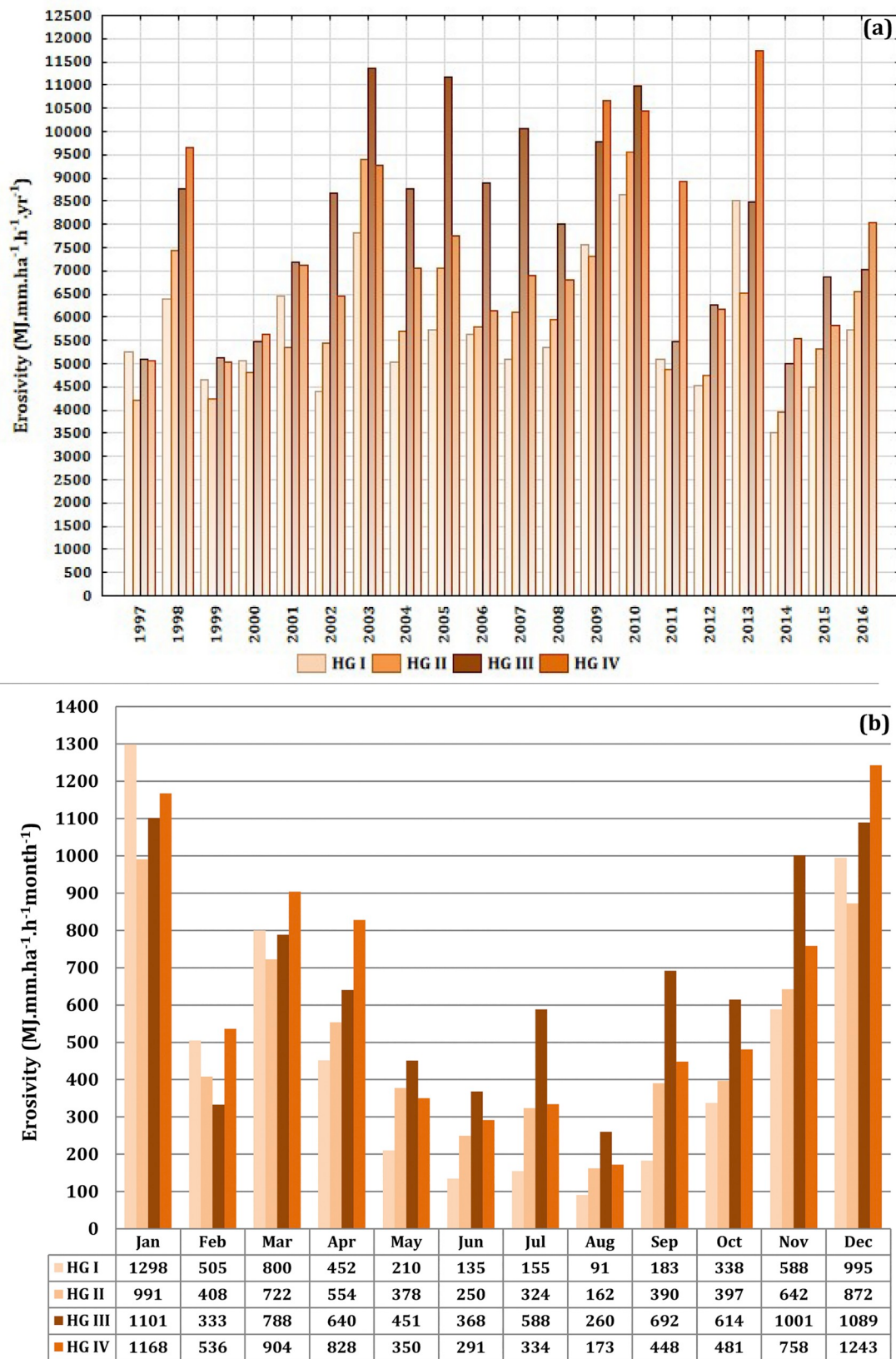


Fig. 13. Annual (a) and monthly (b) distribution of the erosivity estimates in the homogeneous groups of the city of Rio de Janeiro.

should be noted that the highest total annual values of erosivity for HGIII are attributable mainly to the fact that this sector shows higher values between May and November, when compared to other groups where erosivity significantly reduces in the same period ([Fig. 11b](#)).

4. Conclusions

The results allow the sectorial classification of greater and reduced risk areas to erosive potential in the city of Rio de Janeiro, being essential in socioenvironmental evaluations and for the prediction of human, social and economic losses. The statistical procedures applied reveal an annual cycle of rainfall that is directly associated with physiographic aspects such as sea level and orography, while the monthly distribution of rainfall is more related to regional atmospheric dynamics. ([Figs. 12 and 13](#))

It is verified that the municipality of Rio de Janeiro has a high space-time variability of rainfall and erosivity. It was identified that the greatest rainfall for the MRJ does not necessarily occur in higher elevations (HGIII), but in conditions of high population density and formation of urban heat islands, a scenario that favors the increase of convective activity and intense rainfall and, consequently, higher erosivity.

Both the spatialization method and cluster analysis (Ward's method) indicated that the sectors of higher altitudes of the Gericinó, Pedra Branca and Tijuca massifs (orographic effect), which receive high annuals and monthly rainfall totals, are the sectors with higher erosive potential. The same applies to HGIV, which associated to greater slopes, shallow soils and the disordered occupation, indicates a high susceptibility to mass movements and erosive processes.

It was perceived that the HGI corresponds to the sector of minimum rainfall totals in MRJ, mainly because it is located in leeward of the Pedra Branca and Tijuca massifs, which makes it difficult to form rainfall in this sector and reduces erosivity potential. It is worth noting the effect of sea level, specifically for the reduction of rainfall and erosivity in the months of the dry season (April to August), especially for HG II, a sector in which even at low altitudes, the abrupt variation of topography combined with high insolation and high sea surface temperature can ensure high stability of the underlying air and, under favorable synoptic conditions, generate convective instability.

The period between September and April concentrates 85.7% of the erosive potential related to rainfall, being the months of January and December the periods of greater erosivity. The frequent occurrence of dry spells in February and the scarcity of rainfall in August show that these months are indeed influential in reducing the erosive potential in MRJ. This concentration of rainfall and erosivity reveal characteristics inherent to the tropical climate of Central Brazil, as this sector of the national territory presents a significant singularity in the occurrence of rainfall predominantly in the spring and summer months.

Descriptive statistics indicate that the HG I and III have the largest rainfall variance, with standard deviations and quartile intervals indicating that HGI has a predominance of the minimum values. These same statistical parameters show the dominance of the maximum values for HGIII. The Bartlett test shows statistical significance for all months in all pluviometric stations in the city of Rio de Janeiro, while the Shapiro-Wilk test indicates the predominance of non-significant results for the months of February and November. Rainfall and erosivity during these two months are influenced by the transition period between the rainy and dry season. Absolute majority of rainfall stations with significant results was identified for the months of April and August, by the constant performance of the FS in the generation of rainfall in MRJ.

Declaration of Competing Interest

Paulo Miguel de Bodas Terassi elaborated the cartograms and graphs and wrote a greater part of the results and discussions, introduction and conclusion;

José Francisco de Oliveira-Júnior, Givanildo de Gois, Antonio Carlos da Silva Oscar Júnior, Bruno Serafini Sobral and Washington Luiz Félix Correia Filho supported the statistical analysis of the results and the writing of the methodological procedures;

Claudio José Cavalcante Blanco, Hamza Vijith and Vitor Hugo Rosa Biffi collaborated in the conceptual review and discussion of the results.

References

- Almeida, C.O.S., Amorim, R.S.S., Eltz, F.L.F., Couto, E.G., Jordani, A.S., 2012. Erosividade da chuva em municípios do Mato Grosso: distribuição sazonal e correlações com dados pluviométricos. Rev. Bras Eng. Agr. Amb. <https://doi.org/10.1590/S141543662012000200003>.
- Álvares, C.A., Stape, J.L., Sentelhas, P.C., De Moraes Gonçalves, J.L., Sparovek, G., 2013. Köppen's climate classification map for Brazil. Meteor Zeitschrif. <https://doi.org/10.1127/0941-2948/2013/0507>.
- Amorim, M.C.C.T., Monteiro, A., 2010. Episódios extremos de precipitação e fragilidade dos ambientes urbanos: exemplos de Portugal e do Brasil. Territorium. https://doi.org/10.14195/1647-7723.17_1.
- André, R., Marques, V., Pinheiro, F., Ferraudo, A., 2008. Identificação de regiões pluviometricamente homogêneas no estado do Rio de Janeiro, utilizando-se valores mensais. Rev. Bras. Met. <https://doi.org/10.1590/S0102-77862008000400009>.
- Armond, N.B., Sant'anna Neto, J.L., 2017. Entre eventos e episódios: ritmo climático e excepcionalidades para uma abordagem geográfica do clima no município do Rio de Janeiro. Rev. Bras. Clim. <https://doi.org/10.5380/abclima.v20i0.49792>.
- Back, A.J., Alberton, J.V., Poletto, C., 2018. Erosivity index and characteristics of erosive rainfall from the Far western region of Santa Catarina, Brazil. J. Environ. Eng. (<http://dx.doi.org/10.1018/04018049-04018049-12>).
- Bazzano, M.G.P., Eltz, F.L.F., Cassol, E.A., 2007. Erosividade, coeficiente de chuva, padrões e período de retorno das chuvas de Quaraí. RS. Rev Bras Cie Solo. <https://doi.org/10.1590/S0100-06832007000500036>.
- Bazzano, M.G.P., Eltz, F.L.F., Cassol, E.A., 2010. Erosividade e características hidrológicas das chuvas de Rio Grande (RS). Rev Bras Ciência Solo. <https://doi.org/10.1590/S0100-06832010000100024>.

- Bernardes, L.M.C., 1953. Tipos de clima do estado do Rio de Janeiro. *Rev. Bras. Geogr.* 9, 727–739.
- Borsato, V.A., Mendonça, F.A., 2015. Participação da massa polar atlântica na dinâmica dos sistemas atmosféricos no Centro Sul do Brasil. Mercator. <https://doi.org/10.4215/RM2015.1401.0008>.
- Brandão, A.M.P.M., 1987. Tendências e oscilações climáticas na área metropolitana do Rio de Janeiro. In: *Dissertação (Mestrado)*, Faculdade de Filosofia, Letras e Ciências Humanas. Universidade de São Paulo.
- Brandão, A.M.P.M., 1996. O Clima Urbano da Cidade do Rio de Janeiro. Tese (Doutorado). In: *Faculdade de Filosofia, Letras e Ciências Humanas*. Univesidade de São Paulo.
- Brito, T.T., Oliveira-Júnior, J.F., Lyra, G.B., Gois, G., Zeri, M., 2016. Multivariate analysis applied to monthly rainfall over Rio de Janeiro state. *Brazil. Met. Atm. Phys. (Print)*. <https://doi.org/10.1007/s00703-016-0481-x>.
- Carvalho, J.R.P., Assad, E.D., 2005. Análise espacial da precipitação pluviométrica no estado de São Paulo: comparação de métodos de interpolação. *Eng. Agr.* <https://doi.org/10.1590/S0100-69162005000200011>.
- Carvalho, L.M.V., Jones, C., Leibmann, B., 2004. The South Atlantic convergence zone: intensity, form, persistence, and relationships with intraseasonal to interannual activity and extreme rainfall. *J. Clim.* [https://doi.org/10.1175/1520-0442\(2004\)017<0088:TSACZI>2.0.CO;2](https://doi.org/10.1175/1520-0442(2004)017<0088:TSACZI>2.0.CO;2).
- Carvalho, D.F., Khoury Júnior, J.K., Varella, C.A.A., Giori, J.K., Machado, R.L., 2012. Rainfall erosivity for the state of Rio de Janeiro estimated by artificial neural network. *Eng. Agr.* <https://doi.org/10.1590/S0100-69162012000100020>.
- Cataldi, M., Assad, L.P.F., Torres Júnior, A.R., Alves, J.L.D., 2010. Estudo da influência das anomalias da TSM do Atlântico sul extratropical na região da CONFLUÊNCIA Brasil Malvinas no regime hidrometeorológico de verão do sul e sudeste do Brasil. *Rev. Bras. Met.* <https://doi.org/10.1590/S0102-77862010000400010>.
- Costa, C.E.A.S., Blanco, C.J.C., 2018. Influência da variabilidade climática sobre a erosividade em Belém (PA). *Rev. Bras. Meteorol.* <https://doi.org/10.1590/0102-7786333010>.
- Cupolillo, F., 2015. *Diagnóstico Hidroclimatológico da Bacia do Rio Doce*. (Saarbrücken).
- Cupolillo, F., Abreu, M.L., Vianello, R.L., 2008. *Climatologia da Bacia do Rio Doce e sua Relação com a Topografia Local*. (Geografias).
- Dereczynski, C.P., Oliveira, J.S., Machado, C.O., 2009. Climatologia da precipitação no município do Rio de Janeiro. *Rev. Bras. Met.* <https://doi.org/10.1590/S0102-7786200900010000>.
- Dubreuil, V., Fante, K.P., Plachon, O., Sant'anna Neto, J.L., 2017. Les types de climats annuels au Brésil: une application de la classification de Köppen de 1961 à 2015. *EchoGéo*. <https://doi.org/10.4000/echogeo.15017>.
- Everitt, B.S., Dunn, G., 1991. *Applied Multivariate Analysis*. Edward Arnold, London.
- Fialho, E.S., Brandão, A.M.P.M., 2000. As chuvas e a (Des) ORGANIZAÇÃO do espaço urbano Carioca. *Geouerj* 4 pp.99-53.
- Foster, G.R., McColl, D.K., Renard, K.G., Moldenhauer, W.C., 1981. Conversion of the universal soil loss equation to SI metric units. *J. Soil Water Conserv.* 36, 355–359.
- Gois, G., Delgado, R.C., Oliveira-Júnior, J.F., 2015. Modelos teóricos transitivos aplicados na interpolação espacial do standardized precipitation index (SPI) para os episódios de El Niño forte no estado do Tocantins, Brasil. *Irriga*. <https://doi.org/10.15809/irriga.2015v20n2p371>.
- Gonçalves, F.A., Silva, D.D., Pruski, F.F., Carvalho, D.F., Cruz, E.S., 2006. Índices e espacialização da erosividade das chuvas para o estado do Rio de Janeiro. *Rev. Bras. Eng. Agr. Amb.* <https://doi.org/10.1590/S1415-43662006000200004>.
- Grimm, A.M., Tedeschi, R.G., 2009. ENSO and extreme rainfall events in South America. *J. Clim.* <https://doi.org/10.1175/2008JCLI2429.1>.
- Hoyos, N., Waylen, P., Jaramillo, A., 2005. Seasonal and spatial patterns of erosivity in a tropical watershed of the Colombian. *J. Hidrol.* <https://doi.org/10.1016/j.jhydrol.2005.03.014>.
- IBGE (Instituto Brasileiro de Geografia e Estatística), 2018. Cidades. Disponível em: <<http://www.ibge.gov.br>>. Acess in 13 march 2018.
- Inmet (Instituto Nacional de Meteorologia), 2018. Normais Climatológicas do Brasil. Available in: <<http://www.inmet.gov.br/portal/index.php?r=clima/normaisclimatologicas>>. Acess in 06 march 2018.
- Keller Filho, T., Assad, E.D., Lima, P.R.S.R., 2005. Regiões pluviometricamente homogêneas no Brasil. *Pesq. Agrop. Brasileira*. <https://doi.org/10.1590/S0100-204X2005000400001>.
- Kousky, V.E., 1988. Pentad outgoing longwave radiation climatology for the South American sector. *Rev. Bras. Met.* 3, 217–231.
- Kubrusly, L.S., 2001. Um procedimento para calcular índices a partir de uma base de dados multivariados. *Pesq Operacdoi*. <https://doi.org/10.1590/S01017438200100010007>.
- Lyra, G.B., Oliveira-Júnior, J.F., Zeri, M., 2014. Cluster analysis applied to the spatial and temporal variability of monthly rainfall in Alagoas state. Northeast of Brazil. *Int. J. Climat.* <https://doi.org/10.1002/joc.3926>.
- Ma, X., Yandong, H., Xu, J., Van Noordwijk, M., Lu, X., 2012. Spatial and temporal variation in rainfall erosivity in a Himalayan watershed. *Catena*. <https://doi.org/10.1016/j.catena.2014.05.017>.
- Mello, Y.R., Oliveira, T.M.N., 2016. Análise estatística e geoestatística da precipitação média para o município de Joinville (SC). *Rev. Bras. Met.* <https://doi.org/10.1590/0102-778631220150040>.
- Mello, C.R., Sá, M.A.C., Curi, N., Mello, J.M., Viola, M.R., 2007. Erosividade mensal e anual da chuva no Estado de Minas Gerais. *Pesq. Agrop. Brasileira*. <https://doi.org/10.1590/S0100-204X2007000400001>.
- Mello, C.R., Viola, M.R., Curi, N., Silva, A.M., 2012. Distribuição espacial da precipitação e da erosividade da chuva mensal e anual no Estado do Espírito Santo. *Rev. Bras. Cie. Solo*. <https://doi.org/10.1590/S0100-06832012000600022>.
- Mello, C.R., Viola, M.R., Beskow, S., Norton, L.D., 2013. Multivariate models for annual rainfall erosivity in Brazil. *Geoderma*. <https://doi.org/10.1016/j.geoderma.2013.03.009>.
- Montebeller, C.A., Ceddia, M.B., Carvalho, D.F., Vieira, S.R., Franco, E.M., 2007. Variabilidade espacial do potencial erosivo das chuvas no Estado do Rio de Janeiro. *Eng. Agric.* <https://doi.org/10.1590/S0100-69162007000300011>.
- Moraes, N.O., Marton, E., Pimentel, L.C.G., 2005. *Simulações numéricas da formação de Ilha de Calor na Região Metropolitana do Rio de Janeiro*. Anua Inst Geoc UFRJ 28 (2), 116–138.
- Noaa/Cpc National Oceanic and Atmospheric Administration/Climate Prediction Center, 2018. Disponível in. http://www.cpc.ncep.noaa.gov/products/analysis_monitoring/ensostuff/ensoyears.shtml Access in 17 July 2015.
- Oliveira, L.F.C., Fiorese, A.P., Medeiros, A.M.M., Silva, M.A.S., 2010. Comparação de metodologias de preenchimento de falhas em séries históricas de precipitação pluvial anual. *Rev. Bras. Eng. Agric. Amb.* <https://doi.org/10.1590/S1415-436620100001100008>.
- Oliveira, P.T.S., Wendland, E., Nearing, M.A., 2013. Rainfall erosivity in Brazil: a review. *Catena*. <https://doi.org/10.1016/j.catena.2012.08.006>.
- Oliveira-Júnior, J.F., Souza, J.C.S., Dias, F.O., Gois, G., Gonçalves, I.F.S., Silva, M.S., 2013. Caracterização do regime de vento no município de Seropédica, Rio de Janeiro (2001 – 2010). *Flor Amb.* <https://doi.org/10.4322/floram.2013.040>.
- Oliveira-Júnior, J.F., Delgado, R.C., Gois, G., Lannes, A., Dias, F.O., Souza, J.C.S., Souza, M., 2014. Análise da precipitação e sua relação com sistemas meteorológicos em Seropédica. Rio de Janeiro. *Flor Amb.* <https://doi.org/10.4322/floram.2014.030>.
- Oscar Júnior, A.C.S., 2018. *Governança territorial em nível metropolitano e risco da mudança climática no Rio de Janeiro*. Tese (Doutorado). Instituto de Geociências, Universidade Estadual de Campinas.
- Panagos, P., Borelli, P., Meusburguer, K., Yu, B., Klik, A., Jae Lim, K., Yang, J.E., Ni, J., Miao, C., Chattopadhyay, N., Sadeghi, S.H., Hazbavi, Z., Zabihi, M., Larionov, G.A., Krasnov, S.F., Gorobets, A.V., Levi, Y., Erpul, G., Birkel, C., Hoyos, N., Naipal, V., Oliveira, P.T.S., Bonilla, C.A., Meddi, M., Nel, W., Al Dashti, H., Boni, M., Diodato, N., Van Oost, K., Nearing, M., Ballabio, C., 2017. Global rainfall erosivity assessment based on high-temporal resolution rainfall records. *Nature*. <https://doi.org/10.1038/s41598-017-04282-8>.
- Quadro, M.F.L., Silva Dias, M.A.F., Herdies, D.L., Gonçalves, L.G.G., 2012. Análise climatológica da precipitação e do transporte de umidade na região da ZCAS através da nova geração de reanálises. *Rev. Bras. Met.* <https://doi.org/10.1590/S0102-778620120000200004>.
- R Core Team, 2016. R: A Language and Environment for Statistical Computing. R Foundation for Statistical Computing, Vienna, Austria. URL Available in: <https://www.R-project.org/>. Access in: 12 set. 2016.

- Reboita, M.S., Gan, M.A., Rocha, R.P., Ambrizzi, T., 2010. Regimes de precipitação na América do Sul. Rev. Bras. Met. <https://doi.org/10.1590/S0102-77862010000200004>.
- Sant'Anna Neto, J.L., 1995. A erosividade das chuvas no estado de São Paulo. Revista do Departamento de Geografia (USP). <https://doi.org/10.7154/RDG.1995.0009.0004>.
- Satyamurty, P., Mattos, L.F., 1989. Climatological lower tropospheric frontogenesis in the midlatitudes due to horizontal deformation and divergence. Mon. Weather Rev. 117 (6), 1355–1364. [https://doi.org/10.1175/1520-0493\(1989\)117<1355:CLTFIT>2.0.CO;2](https://doi.org/10.1175/1520-0493(1989)117<1355:CLTFIT>2.0.CO;2).
- Satyamurty, P., Nobre, C.A., Silva Dias, P.L., 1998. Tropics-South America. In: Kauly, D.J., Vincent, D.G. (Eds.), Meteorology of the Southern Hemisphere. Meteor Monog - Amer Met Soc.
- Schick, J., Bertol, I., Cogo, N.P., González, A.P., 2014. Erosividade das chuvas em Lages. Santa Catarina. Rev Bras Cie Solo. <https://doi.org/10.1590/S0100-06832014000600024>.
- Schlee, M.B., Tamminga, K.R., Tângari, V.R., 2012. A method for gauging landscape change as a prelude to urban watershed regeneration: the case of the Carioca river, Rio de Janeiro. Sustainability 4, 2054–2098. <https://doi.org/10.3390/su4092054>.
- Seluchi, M.E., Chou, S.C., 2009. Synoptic patterns associated with landslides events in the Serra Do Mar. Brazil. Theor Appl Climat. <https://doi.org/10.1007/s00704-008-0101-x>.
- Serra, A.B., 1970. Clima da Guanabara. Bol Geogr. 214, 80–111.
- Serra, A.B., Ratibonha, L., 1957. Clima do Rio de Janeiro. Bol Geogr. 2, 527–560.
- Shamshad, A., Azhari, M.N., Isa, M.H., Wan Hussinw, M.A., Parida, B.P., 2008. Development of an appropriate procedure for estimation of RUSLE EI30 index and preparation of erosivity maps for Pulau Penang in peninsular Malaysia. Catena. <https://doi.org/10.1016/j.catena.2007.08.002>.
- Shastri, H., Paul, S., Gosh, S., Kärmä, S., 2015. Impacts of urbanization on Indian summer monsoon rainfall extremes. J. Geoph. Res. (Atmosph). <https://doi.org/10.1002/2014JD022061>.
- Silva, A.M., 2004. Rainfall erosivity map for Brazil. Catena. <https://doi.org/10.1016/j.catena.2003.11.006>.
- Silva, M.A., Silva, M.I.N., Curi, N., Santos, G.R., Marques, J.J.G.S.M., Menezes, M.D., Leite, F.P., 2010. Avaliação e espacialização da erosividade da chuva no Vale do rio Doce, região Centro-Leste do Estado de Minas Gerais. Rev Bras Cie Solo. <https://doi.org/10.1590/S0100-06832010000400003>.
- Silva, A.M., Wiecheteck, M., Zuercher, B.W., 2011. Spatial assessment of indices for characterizing the erosive force of rainfall in El Salvador Republic. Environ. Eng. Sci. <https://doi.org/10.1089/ees.2010.0296>.
- Sobral, B.S., Oliveira-Júnior, J.F., Gois, G., Terassi, P.M.B., Muniz-Júnior, J.G.R., 2018. Variabilidade Espaço-temporal e interanual da chuva no estado do Rio De Janeiro. Rev. Bras. Climat. <https://doi.org/10.5380/abclima.v22i0.55592>.
- Souza, W.M., Azevedo, P.V., Araújo, L.E., 2012. Classificação da precipitação diária e impactos decorrentes dos desastres associados às chuvas na cidade do Recife - PE. Rev. Bras Geo. Fis. 2, 250–268.
- Terassi, P.M.B., Oliveira-Júnior, J.F., Gois, G., Galvani, E., 2018. Variabilidade do índice de precipitação padronizada na Região Norte do Estado do Paraná Associada aos Eventos de El Niño-Oscilação Sul. Rev. Bras. Met. <https://doi.org/10.1590/0102-7786331002>.
- Trindade, A.L.F., Oliveira, P.T.S., Anache, J.A.A., Wendland, E., 2016. Variabilidade espacial da erosividade das chuvas no Brasil. Ver Pesq Agrop. <https://doi.org/10.1590/s0100-204x2016001200002>.
- Villela, S.M., Mattos, A., 1975. Hidrologia aplicada. McGraw-Hill do Brasil, São Paulo.
- Waltrick, P.C., Machado, M.A.M., Dieckow, J., Oliveira, D., 2015. Estimativas da erosividade de chuvas no estado do Paraná pelo método da pluviometria: Atualização com dados de 1986 a 2008. Rev Bras Cie Solo. <https://doi.org/10.1590/01000683rbcs20150147>.
- Ward, J.H., 1963. Hierarchical grouping to optimize an objective function. Journal of the American Statistical Association 58, 236–244. <https://doi.org/10.1080/01621459.1963.10500845>.
- Zandonadi, L., Acquaotta, F., Fratianni, S., Zavattini, J.A., 2015. Changes in precipitation extremes in Brazil (Paraná River basin). Theor. Appl. Climatol. <https://doi.org/10.1007/s00704-015-1391-4>.
- Zanella, M.E., 2006. Eventos pluviométricos intensos e impactos gerados na cidade de Curitiba/PR - Bairro Cajuru: um destaque para as inundações urbanas. Mercator. <https://doi.org/10.4215/RM0000.0000.0000>.
- Zanella, M.E., Salles, M.C.L., 2016. Impactos pluviais em Fortaleza – CE na perspectiva do sistema Clima Urbano. Rev. Bras. Geo. Fis. <https://doi.org/10.5935/1984-2295.20160163>.
- Zeri, M., Oliveira-Júnior, J.F., Lyra, G.B., 2011. Spatiotemporal analysis of particulate matter, sulfur dioxide and carbon monoxide concentrations over the city of Rio de Janeiro. Brazil. Meteor Atmosph Phys (Print). <https://doi.org/10.1007/s00703-011-0153-9>.